

The Seasonal Cycle of pCO₂ and CO₂ fluxes in the Southern Ocean: Diagnosing Anomalies in CMIP5 Earth Systems Models

Precious N. Mongwe^{1,2}, Marcello Vichi^{2,3} & Pedro M.S. Monteiro^{1,2}

¹Southern Ocean Carbon-Climate Observatory (SOCCO), CSIR, Cape Town, South Africa

²Department of Oceanography, University of Cape Town, Cape Town, South Africa

³Marine Research Institute, University of Cape Town, Cape Town, South Africa

pmongwe@csir.co.za

Abstract

The Southern Ocean forms an important component of the global carbon cycle as a sink of CO₂ and heat. Recent studies based on the Coupled Model Intercomparison Project version 5 (CMIP5) Earth System Models (ESMs) show that CMIP5 models disagree on the phasing of the seasonal cycle of the CO₂ flux (FCO₂) and poorly compare with available observations estimates in the Southern Ocean. Because the seasonal cycle is the dominant mode of CO₂ variability in the Southern Ocean, its proper simulation is necessary to model long-term oceanic CO₂ changes and their related climate impacts. Here we examine the competing roles of temperature and dissolved inorganic carbon (DIC) as drivers of the seasonal cycle of pCO₂ in the Southern Ocean to explain the mechanistic basis for the seasonal biases in CMIP5 models, comparing them with observational products. We find that despite significant differences in the spatial characteristics of the mean annual fluxes, models show greater zonal homogeneity in the seasonal cycle of FCO₂ than observational products. The CMIP5 models can be grouped into one or the other of two main categories (group-SST and group-DIC) while observational products show a modest influence of both, with a dominance of DIC changes as the main driver of seasonal FCO₂ variability. Group-SST models show an exaggeration of the seasonal rates of change of sea surface temperature (SST) in autumn and spring during the cooling and warming peaks. The higher-than-observed rates of SST change tip the control of the seasonal cycle of pCO₂ and FCO₂ towards SST and result in a divergence between the observed and modelled seasonal cycles, particularly in the Sub-Antarctic Zone. While almost all analysed models (9 out of 10) show these SST-driven biases, 3 out of 10 (namely NorESM1-ME, HadGEM-ES and MPI-ESM, collectively the group-DIC models) compensate the solubility bias because of their overly-exaggerated primary production, such that biologically-driven DIC changes mainly regulate the seasonal cycle of FCO₂. Group-DIC models reproduce the observed phasing of FCO₂ as a result of an incorrect scaling of the biogeochemical fluxes. In the Antarctic zone, CMIP5 models compare better with observations relative to

Style Definition ... [3]

V2 Changes 2018/3/6 6:53 PM

Deleted: Mechanisms of the Sea-Air ... [4]

V2 Changes 2018/3/6 6:53 PM

Formatted ... [5]

V2 Changes 2018/3/6 6:53 PM

Deleted: biases...f pCO₂ and CO₂ flux ... [6]

V2 Changes 2018/3/6 6:53 PM

Deleted: N. Precious^{1,2}, Vichi ... [7]

V2 Changes 2018/3/6 6:53 PM

Deleted: ²Oceanography Department ... [8]

V2 Changes 2018/3/6 6:53 PM

Deleted: pmongwe@csir.co.za -

V2 Changes 2018/3/6 6:53 PM

Formatted ... [9]

V2 Changes 2018/3/6 6:53 PM

Formatted ... [10]

V2 Changes 2018/3/6 6:53 PM

Formatted ... [11]

V2 Changes 2018/3/6 6:53 PM

Formatted ... [12]

V2 Changes 2018/3/6 6:53 PM

Deleted: a key

V2 Changes 2018/3/6 6:53 PM

Deleted: .

V2 Changes 2018/3/6 6:53 PM

Formatted ... [13]

V2 Changes 2018/3/6 6:53 PM

Formatted ... [14]

V2 Changes 2018/3/6 6:53 PM

Deleted: , however, show that CMIP5

V2 Changes 2018/3/6 6:53 PM

Formatted ... [15]

V2 Changes 2018/3/6 6:53 PM

Deleted: ESM)

V2 Changes 2018/3/6 6:53 PM

Formatted ... [16]

V2 Changes 2018/3/6 6:53 PM

Deleted: representation

V2 Changes 2018/3/6 6:53 PM

Formatted ... [17]

V2 Changes 2018/3/6 6:53 PM

Deleted: poorly to

V2 Changes 2018/3/6 6:53 PM

Formatted ... [18]

V2 Changes 2018/3/6 6:53 PM

Deleted: This

V2 Changes 2018/3/6 6:53 PM

Formatted ... [19]

V2 Changes 2018/3/6 6:53 PM

Deleted: -observations bias has imp ... [20]

V2 Changes 2018/3/6 6:53 PM

Formatted ... [21]

V2 Changes 2018/3/6 6:53 PM

Deleted: feedbacks. In this study,

V2 Changes 2018/3/6 6:53 PM

Deleted: used a specialized diagnos ... [23]

V2 Changes 2018/3/6 6:53 PM

Formatted ... [22]

V2 Changes 2018/3/6 6:53 PM

Formatted ... [24]

V2 Changes 2018/3/6 6:53 PM

Formatted ... [25]

V2 Changes 2018/3/6 6:53 PM

Formatted ... [26]

V2 Changes 2018/3/6 6:53 PM

Formatted ... [27]

V2 Changes 2018/3/6 6:53 PM

Formatted ... [28]

V2 Changes 2018/3/6 6:53 PM

101 [the Sub-Antarctic Zone](#). This is mostly because both the [CMIP5 models](#) and the [observational product](#) show
102 [a spatial and temporal uniformity in the characteristics of FCO₂ in the Antarctic zone](#). It is unfortunately not
103 [possible to assess if CMIP5 models effectively perform better in this region or if the observational products](#)
104 [are limited by the lack of *in situ* data](#). The [suggested mechanisms should be investigated further with CMIP6](#)
105 [models and new available data from autonomous platforms, and our analysis framework is proposed as a](#)
106 [useful tool to diagnose the dominant drivers](#).

V2 Changes 2018/3/6 6:53 PM
Deleted: influence of these two extremes, observations show a modest influence of both, with a dominance of DIC regulation. We found that CMIP5 models overestimate cooling and warming rates during autumn and spring with respect to observations. Because of this, the role of solubility is overestimated, particularly during these seasons (autumn and spring) in group B models, to the extent of contradicting the biological CO₂ uptake during spring. Group A does not show this solubility driven bias due to the overestimation of DIC draw down. This finding strongly implies that the inability of the CMIP5 ESMs to resolve CO₂ biological uptake during spring might be crucially related to the sensitivity of the pCO₂ to temperature in addition to underestimated biological CO₂ uptake.

108 1. Introduction

109
110 [The Southern Ocean \(south of 30°S\) takes up about a third of the total oceanic CO₂ uptake, slowing down](#)
111 [the accumulation of CO₂ in the atmosphere \(Fung et al., 2005; Le Quere et al., 2016; Takahashi et al., 2012\)](#).
112 [The combination of upwelling deep ocean circumpolar waters \(which are rich in carbon and nutrients\) and](#)
113 [the subduction of fresh-colder mid-latitude waters makes it a key region in the role of sea-air gas exchange](#)
114 [and heat \(Barbero et al., 2011; Gruber et al., 2009; Sallée et al., 2013\)](#). The Southern Ocean supplies about
115 [a third of the total nutrients responsible for biological production north of 30°S \(Sarmiento et al., 2004\)](#),
116 [and accounts for about 75% of total ocean heat uptake \(Frölicher et al., 2015\)](#). Recent studies suggests that
117 [the Southern Ocean CO₂ sink is expected to change as result of anthropogenic warming, however, the sign](#)
118 [and magnitude of the change is still disputed \(Leung et al., 2015; Roy et al., 2011; Sarmiento et al., 1998;](#)
119 [Segsneider and Bendtsen, 2013\)](#). While some studies suggest that the Southern Ocean CO₂ sink is
120 [weakening and will continue to do so \(e.g. Le Quéré et al., 2007; Son and Gerber, 2010; Thompson et al.,](#)
121 [2011\)](#), other recent studies infer an increasing CO₂ sink (Landschutzer et al., 2015; Takahashi et al., 2012;
122 [Zickfeld et al., 2008\)](#).

V2 Changes 2018/3/6 6:53 PM
Deleted: [31]

V2 Changes 2018/3/6 6:53 PM
Formatted: Font: 11 pt, Not Bold

V2 Changes 2018/3/6 6:53 PM
Deleted: The Southern Ocean takes up about a third of the total oceanic CO₂ uptake, slowing down the accumulation of CO₂ in the atmosphere (Fung et al., 2005; Le Quere et al., 2016; Takahashi et al., 2012). The combination of upwelling deep ocean circumpolar waters, rich in carbon and nutrients, and the subduction of fresh and colder mid-latitude waters makes it a key region in the role of sea-air exchange (Barbero et al., 2011; Gruber et al., 2009; Sallée et al., 2013). The Southern Ocean supplies about a third of the total nutrients responsible for biological production north of 30°S (Sarmiento et al., 2004), and accounts for about 75% of total oceanic heat uptake (Frölicher et al., 2015). The century scale evolution of the Southern Ocean CO₂ ... [32]

124 Although the Southern Ocean plays a crucial role as a CO₂ reservoir and regulator of nutrients and heat, it
125 remains under-sampled, especially during the winter season ([JJA, Australian annual cycle](#)) (Bakker et al.,
126 2014; Monteiro et al., 2010). [Consequently](#) we largely rely on Earth System Models (ESM), inversions and
127 ocean models for both process understanding and future simulation of CO₂ processes in the Southern
128 Ocean. The Coupled Model Intercomparison Project (CMIP) provides an example of such a globally
129 organized platform (Taylor et al., 2012). Recent studies based on CMIP5 ESMs, forward and inversions
130 models show that [CMIP5 models agree on the CO₂ annual mean sink](#), they disagree [with available](#)
131 [observations](#) on the [phasing of the seasonal cycle of sea-air CO₂ flux \(FCO₂\) in the Southern Ocean](#) (e.g.
132 Anav et al., 2013; Lenton et al., 2013).

V2 Changes 2018/3/6 6:53 PM
Formatted: normal

V2 Changes 2018/3/6 6:53 PM
Deleted: Thus,

V2 Changes 2018/3/6 6:53 PM
Deleted: although

V2 Changes 2018/3/6 6:53 PM
Deleted: in the Southern Ocean

V2 Changes 2018/3/6 6:53 PM
Deleted: and they are out of phase with observations

V2 Changes 2018/3/6 6:53 PM
Deleted:

V2 Changes 2018/3/6 6:53 PM
Formatted: ... [30]

V2 Changes 2018/3/6 6:53 PM
Formatted: Default Paragraph Font

210 The seasonal cycle is a major mode of variability for chlorophyll (Thomalla et al., 2011) and CO₂ in the
211 Southern Ocean (Monteiro et al., 2010; Lenton et al., 2013). The large-scale seasonal states of sea-air CO₂
212 fluxes (FCO₂) in the Southern Ocean comprise of extremes of strong summer ingassing with a weaker
213 ingassing or even outgassing in winter (Metzl et al., 2006). These extremes are linked by the autumn and
214 spring transitions. In autumn CO₂ ingassing weakens linked to the increasing entrainment of sub-surface
215 waters, which are rich in dissolved inorganic carbon (DIC), (Lenton et al., 2013; Metzl et al., 2006;
216 Sarmiento and Gruber, 2006). During spring, the increase of primary production consumes DIC at the
217 surface and increases the ocean capacity to take up atmospheric CO₂ (Gruber et al., 2009; Le Quéré and
218 Saltzman, 2013; Pasquer et al., 2015; Gregor et al., 2017). The increase of sea surface temperature (SST) in
219 summer reduces surface CO₂ solubility, which counteracts the biological uptake and reduces the CO₂ flux
220 from the atmosphere (Takahashi et al., 2002; Lenton et al., 2013).

221
222 FCO₂ is also spatially variable in the Southern Ocean at the seasonal scale. North of 50°S is generally the
223 main CO₂ uptake zone (Hauck et al., 2015; Sabine et al., 2004). This region forms a major part of the sub-
224 Antarctic zone and is characterized by the confluence of upwelled, colder and nutrient-rich deep
225 circumpolar water and mid-latitudes warm water (McNeil et al., 2007; Sallée et al., 2006) . It is
226 characterized by enhanced biological uptake during spring and solubility driven CO₂ uptake due to cool
227 surface waters (Marinov et al., 2006; Metzl, 2009; Takahashi et al., 2012). South of 60°S towards the
228 marginal ice zone, CO₂ fluxes are largely dominated by outgassing, driven by the upwelling of circumpolar
229 waters, which are rich in DIC (Matear and Lenton, 2008; McNeil et al., 2007).

230
231 The inability of CMIP5 ESM to simulate a comparable FCO₂ seasonal cycle with available observations
232 estimates in the Southern Ocean has been the subject of recent literature (e.g. Anav et al., 2013; Kessler
233 and Tjiputra, 2016) and the mechanisms associated with these biases are still not well understood. This
234 model-observations disagreement highlights that the current ESMs might not adequately capture the
235 dominant seasonal processes driving the FCO₂ in the Southern Ocean. It also questions the sensitivity of
236 models to adequately predict the Southern Ocean century scale CO₂ sink and its sensitivity to climate
237 change feedbacks (Lenton et al., 2013). Efforts to improve simulations of CO₂ properties with respect to
238 observations in the Southern Ocean are ongoing using forced ocean models (e.g. Pasquer et al., 2015;
239 Rodgers et al., 2014; Visinelli et al., 2016; Rosso et al., 2017). However it remains a challenge for fully
240 coupled simulations. In a previous study, we developed a diagnostic framework to evaluate the seasonal
241 characteristics of the drivers of FCO₂ in ocean biogeochemical models (Mongwe et al., 2016). We here
242 apply this approach to 10 CMIP5 models against observation product estimates in the Southern Ocean. The
243 subsequent analysis is divided as follows; the methods section (section 2) explains our methodological

V2 Changes 2018/3/6 6:53 PM
Deleted: the

V2 Changes 2018/3/6 6:53 PM
Deleted: in gassing

V2 Changes 2018/3/6 6:53 PM
Deleted: in-gassing

V2 Changes 2018/3/6 6:53 PM
Deleted: state

V2 Changes 2018/3/6 6:53 PM
Deleted: Ref).

V2 Changes 2018/3/6 6:53 PM
Deleted: in gassing

V2 Changes 2018/3/6 6:53 PM
Deleted:)

V2 Changes 2018/3/6 6:53 PM
Deleted: from September,

V2 Changes 2018/3/6 6:53 PM
Deleted: onset

V2 Changes 2018/3/6 6:53 PM
Deleted: with

V2 Changes 2018/3/6 6:53 PM
Deleted: weakens the

V2 Changes 2018/3/6 6:53 PM
Deleted: ; Pasquer et al., 2015).

V2 Changes 2018/3/6 6:53 PM
Deleted: -

... [33]

V2 Changes 2018/3/6 6:53 PM
Formatted: normal

V2 Changes 2018/3/6 6:53 PM
Deleted: do

V2 Changes 2018/3/6 6:53 PM
Deleted: region

V2 Changes 2018/3/6 6:53 PM
Deleted:), however

V2 Changes 2018/3/6 6:53 PM
Deleted: In this work we applied this method to investigate the processes that drive FCO₂ at the seasonal scale in 10 CMIP5 ESM, exploring the mechanisms of the observed model biases in the Southern Ocean

V2 Changes 2018/3/6 6:53 PM
Formatted: normal, Right, Tabs: 7,62 cm, Centered + 15,24 cm, Right, Position:Horizontal: Left, Relative to: Column, Vertical: In line, Relative to: Margin, Wrap Around

V2 Changes 2018/3/6 6:53 PM
Formatted: Default Paragraph Font

266 [approach, followed by results \(section 3\), which comprise four subsections. Section 3.1 explores the spatial](#)
267 [variability of the annual mean representation of FCO₂ in the 10 CMIP5 models against observation product](#)
268 [estimates; section 3.2 quantitatively the biases in the FCO₂ seasonal cycles in the 10 models. Section 3.3](#)
269 [investigates surface ocean drivers of FCO₂ changes \(temperature driven solubility and primary production\),](#)
270 [and finally section 3.4 examines the source terms in the DIC surface budget \(primary production,](#)
271 [entrainment rates and vertical gradients\) and their role in surface pCO₂ changes. The discussion \(section 4\)](#)
272 [is an examination of the mechanisms behind the pCO₂ and FCO₂ biases in the models. We conclude with a](#)
273 [synthesis of the main findings and implications.](#)

275 2. Methods

277 [The Southern Ocean is here defined as the ocean south of the Sub-Tropical Front \(STF, defined according to](#)
278 [Orsi et al., \(1995\), 11.3°C isotherm at 100m\). It is divided into two main domains, the Sub-Antarctic Zone;](#)
279 [between the STF and the Polar Front \(PF: 2°C isotherm at 200m\) and the Antarctic Zone, south of the PF.](#)
280 [Within the Sub-Antarctic Zone and Antarctic Zone, we further partition the domain into the three main](#)
281 [basins of the Southern Ocean i.e. Pacific, Atlantic and the Indian Ocean.](#)

283 2.1 Observations datasets

284 [We used the Landschützer et al \(2014\) data product \(FCO₂ and partial pressure of CO₂ \(pCO₂\)\) as the main](#)
285 [suite of observations-based estimates against to which compare the models throughout the analysis.](#)
286 [Landschützer et al \(2014\) dataset is synthesized from Surface Ocean CO₂ Atlas version 2 \(SOCAT2\)](#)
287 [observations and high resolution winds using a Self Organizing Map \(SOM\) through a Feed Forward Neural](#)
288 [Network \(FNN\) approach \(Landschützer et al., 2013\). While Landschützer et al \(2014\) dataset is based on](#)
289 [more *in situ* observations \(SOCAT2, 15 million source measurements Bakker et al., 2014\) in comparison to](#)
290 [Takahashi et al., 2009 \(3 million surface measurements\), used in Mongwe et a., \(2016\). We are nevertheless](#)
291 [mindful that due to paucity of observations in Southern Ocean, this data product is still subject to](#)
292 [significant uncertainties discussed in Ritter et al., \(2018\). To evaluate the uncertainty between data](#)
293 [products we compare the Landschützer et al \(2014\) data with Gregor et al \(2017\) data product, which is](#)
294 [based on two independent empirical models: Support Vector Regression \(SVR\) and Random Forest](#)
295 [Regression \(RFR\) as well as against Takahashi et al \(2009\) for pCO₂ in the Southern Ocean. We compare](#)
296 [pCO₂ instead of FCO₂ firstly, because Gregor et al., \(2017\) only provided fugacity and pCO₂, and being](#)
297 [mindful that the choice of wind product and transfer velocity constant in computing FCO₂ would increase](#)
298

V2 Changes 2018/3/6 6:53 PM
Formatted: Font:11 pt, Not Bold

V2 Changes 2018/3/6 6:53 PM
Deleted:

V2 Changes 2018/3/6 6:53 PM
Formatted: Font:14 pt, Bold

V2 Changes 2018/3/6 6:53 PM
Formatted: normal, Indent: Left: 0 cm

V2 Changes 2018/3/6 6:53 PM
Formatted: normal

V2 Changes 2018/3/6 6:53 PM
Moved (insertion) [1]

V2 Changes 2018/3/6 6:53 PM
Deleted: We used the Landschützer et al (2014) FCO₂ and partial pressure of CO₂ (pCO₂) dataset as the main suite of observations to compare against models throughout the analysis. Landschützer et al (2014) data are synthesized from Surface Ocean CO₂ Atlas version 2 (SOCAT2) observations and high resolution winds using neural network techniques (Landschützer et al., 2013). Here we use this dataset as provided by Landschützer et al (2014) on a 1° x 1° regular grid. We also used the Takahashi et al. (2009) *in situ* FCO₂ dataset as a complementary source for comparison of spatial sea-air CO₂ fluxes properties in the Southern Ocean. Takahashi et al., (2009) data are comprised of a compilation of about 3 million surface measurements globally, obtained from 1970 – 2000 and corrected for reference year 2000. This dataset is used, as provided, on a 4° (latitude) x 5° (longitude) resolution. ... [34]

V2 Changes 2018/3/6 6:53 PM
Formatted: normal, Right, Tabs: 7,62 cm, Centered + 15,24 cm, Right, Position: Horizontal: Left, Relative to: Column, Vertical: In line, Relative to: Margin, Wrap Around

V2 Changes 2018/3/6 6:53 PM
Formatted: Default Paragraph Font

322 [the level of uncertainty \(Swart et al., 2014\)](#). Secondly, while the focus of the paper is on the examination
323 [biases in the air-sea flux of CO₂, the major part of our diagnostic analysis is based on pCO₂, which primarily](#)
324 [determines the direction and part of the magnitude of the fluxes. We find that the three data products](#)
325 [agree on the seasonal phasing of pCO₂ in the Sub-Antarctic zone, but they show differences in the](#)
326 [magnitudes \(Fig. S1\). In the Antarctic zone, all three datasets agree in both phasing and amplitude \(Fig. S1\).](#)
327 [At this stage it is not clear whether this agreement is due to all the methods converging even with the](#)
328 [sparse data or the reason for agreement is the lack of observations is reason for the agreement.](#)
329 [Nevertheless more independent in situ observations will be helpful to resolve this issue In this regard float](#)
330 [observations from the SOCCOM program \(Johnson et al., 2017\) and glider observations \(Monteiro et al.,](#)
331 [2015\) for example are likely to become helpful in resolving these data uncertainties in addition to ongoing](#)
332 [ship based measurements.](#)

333
334 [We also used the Takahashi et al. \(2009\) in situ FCO₂ dataset as a complementary source for comparison of](#)
335 [spatial FCO₂ properties in the Southern Ocean. Takahashi et al., \(2009\) data estimates are comprised of a](#)
336 [compilation of about 3 million surface measurements globally, obtained from 1970 – 2000 and corrected](#)
337 [for reference year 2000. This dataset is used, as provided, on a 4° \(latitude\) x 5° \(longitude\) resolution.](#)
338 [Using monthly mean sea surface temperature \(SST\) and salinity from the World Ocean Atlas 2013 \(WOA13\)](#)
339 [dataset \(Locarnini et al., 2013\), we reconstructed total alkalinity \(TAlk\) using the Lee et al. \(2006\)](#)
340 [formulation. We also use this dataset as the main observations platform in section 2.3. To calculate the](#)
341 [uncertainty of the computed TAlk, we compared the calculated total alkalinity \(TAlk_{obs}\) based on ship](#)
342 [measurements of SST and surface salinity dataset with actual observed TAlk_{obs} of the same measurements](#)
343 [for a set of winter \(August\) data collected in the Southern Ocean. We found that TAlk_{calc} compares well with](#)
344 [TAlk_{obs} \(R² = 0.79\) \(Fig. S2, Supplementary\). We then used this computed monthly TAlk and pCO₂ from](#)
345 [Landschützer et al \(2014\) to compute DIC using CO2SYS \(Pierrot et al., 2006,](#)
346 [http://cdiac.ornl.gov/ftp/co2sys/CO2SYS_calc_XLS_v2.1\), using K1, K2 from Mehrbach et al., 1973 refited](#)
347 [by Dickson and Millero, 1987. For interior ocean DIC, we used the Global Ocean Data Analysis Project](#)
348 [version 2 \(GLODAP2\) annual means dataset \(Lauvset et al., 2016\). The Mixed Layer Depth \(MLD\) data was](#)
349 [taken from de Boyer Montégut et al. \(2004\), on a 1° x 1° grid, the data is provided as monthly means](#)
350 [climatology and was used as provided. We also use satellite chlorophyll dataset from Johnson et al., \(2013\).](#)

351
352 **2.2 CMIP5 Model data**
353

V2 Changes 2018/3/6 6:53 PM

Formatted: Font:12 pt, Bold

V2 Changes 2018/3/6 6:53 PM

Formatted: normal, Space After: 8,1 pt

V2 Changes 2018/3/6 6:53 PM

Formatted: normal

V2 Changes 2018/3/6 6:53 PM

Formatted: normal, Right, Tabs: 7,62 cm, Centered + 15,24 cm, Right, Position:Horizontal: Left, Relative to: Column, Vertical: In line, Relative to: Margin, Wrap Around

V2 Changes 2018/3/6 6:53 PM

Formatted: Default Paragraph Font

354 We used 10 models from the Coupled Model Intercomparison Project version 5 (CMIP5) Earth System
 355 Models (ESM) shown in Table 1. The selection criterion for the models was based on the availability of
 356 essential variables for the analysis in the CMIP5 data portal (<http://pcmdi9.llnl.gov>) at the time of writing:
 357 i.e. monthly FCO₂, pCO₂, chlorophyll, net primary production (NPP), surface oxygen, surface Dissolved
 358 Inorganic Carbon (DIC), MLD, Sea Surface Temperature (SST), vertical temperature fields and annual DIC for
 359 the historical scenario. The analysis is primarily based on the climatology over 1995 – 2005, which was
 360 selected to match a period closest to the available observational data product (Landschützer et al (2014),
 361 1998 – 2011). However we do examine the consistency of the seasonality of FCO₂ over periods longer than
 362 10 years by comparing the seasonal cycle of FCO₂ and temporal standard deviation of 30 years (1975 –
 363 2005) vs 10 years (1995 – 2005) for HadGEM2-ES and CanESM2. We find that the seasonal cycle of FCO₂
 364 remains consistent (R = 0.99) in both HadGEM2-ES and CanESM2 over 30 year (Fig. S3). All CMIP5 model
 365 outputs were regridded into a common 1°x1° regular grid throughout the analysis, except for annual CO₂
 366 mean fluxes, which were computed on the original grid for each model.

368 **Table 1:** A description of the 10 CMIP5 ESMs that were used in this analysis. It shows the ocean resolution,
 369 atmospheric resolution, and available nutrients for the biogeochemical component, sea-ice model, vertical
 370 levels and the marine biogeochemical component for each ESM.

Full name and Source	Model Name	Ocean Resolution	Atmospheric Resolution	Nutrients	Sea ice model	Vertical Coordinate & Levels	Ocean Biology	Reference
Canadian Centre for Climate Modelling and Analysis, Canada	CanESM2	CanOM4 0.9° x 1.4°	2.8125° x 2.8125°	N (accounts for Fe limitation)	CanSIM1	z 40 levels	NP2D	Zahariev et al., 2008
Centro Euro-Mediterraneo Sui Cambiamenti Climatici, Italy	CMCC-CESM	OPA8.2 0.5-2°x2°	3.8° x 3.7°	P, N, Fe, Si	CICE4	z 21 levels	PELAGOS	Vichi et al., 2007
Centre National de Recherches Météorologiques-Centre Européen de Recherche et de Formation Avancée en Calcul Scientifique, France	CNRM-CM5	NEMOv3.3 1°	1.4°	P, N, Fe, Si	GELATOS	z 42 levels	PISCES	Séférian et al., 2013

6

Deleted: In this study we

V2 Changes 2018/3/6 6:53 PM
Formatted ... [37]

V2 Changes 2018/3/6 6:53 PM
Deleted: 10 ...oupled Model ... [38]

V2 Changes 2018/3/6 6:53 PM
Deleted: , showing their ... It shows ... [39]

V2 Changes 2018/3/6 6:53 PM
Formatted ... [40]

V2 Changes 2018/3/6 6:53 PM
Formatted ... [42]

V2 Changes 2018/3/6 6:53 PM
Inserted Cells ... [43]

V2 Changes 2018/3/6 6:53 PM
Deleted: Z-

V2 Changes 2018/3/6 6:53 PM
Formatted ... [41]

V2 Changes 2018/3/6 6:53 PM
Inserted Cells ... [44]

V2 Changes 2018/3/6 6:53 PM
Inserted Cells ... [45]

V2 Changes 2018/3/6 6:53 PM
Formatted ... [47]

V2 Changes 2018/3/6 6:53 PM
Formatted ... [48]

V2 Changes 2018/3/6 6:53 PM
Formatted ... [46]

V2 Changes 2018/3/6 6:53 PM
Formatted ... [49]

V2 Changes 2018/3/6 6:53 PM
Formatted ... [50]

V2 Changes 2018/3/6 6:53 PM
Deleted:

V2 Changes 2018/3/6 6:53 PM
Formatted ... [53]

V2 Changes 2018/3/6 6:53 PM
Deleted: Zahariev et al., 2008

V2 Changes 2018/3/6 6:53 PM
Formatted ... [51]

V2 Changes 2018/3/6 6:53 PM
Formatted ... [52]

V2 Changes 2018/3/6 6:53 PM
Formatted ... [54]

V2 Changes 2018/3/6 6:53 PM
Formatted ... [55]

V2 Changes 2018/3/6 6:53 PM
Formatted ... [58]

V2 Changes 2018/3/6 6:53 PM
Deleted: Vichi et al., 2007

V2 Changes 2018/3/6 6:53 PM
Formatted ... [56]

V2 Changes 2018/3/6 6:53 PM
Formatted ... [57]

V2 Changes 2018/3/6 6:53 PM
Formatted ... [63]

V2 Changes 2018/3/6 6:53 PM
Deleted: Séférian et al., 2013

V2 Changes 2018/3/6 6:53 PM
Formatted ... [59]

V2 Changes 2018/3/6 6:53 PM
Formatted ... [60]

V2 Changes 2018/3/6 6:53 PM
Formatted ... [61]

V2 Changes 2018/3/6 6:53 PM
Formatted ... [62]

V2 Changes 2018/3/6 6:53 PM
Formatted ... [35]

V2 Changes 2018/3/6 6:53 PM
Formatted ... [36]

Institut Pierre-Simon Laplace, France	JPSL-CMSA-MR	NEMO2.3 0.5-2° x 2°	2.58° x 1.25°	P, N, Fe, Si	LIM2	z 31 levels	PISCES	Séférian et al., 2013
Max Planck Institute for Meteorology, Germany	MPI-ESM-MR	MPIOM 1.41° x 0.89°	1.875° x 1.875°	P, N, Fe, Si	MPIOM	z 40 levels	HAMOC5.2	Ilyina et al., 2013
Community Earth System Model, USA	CESM1-BGC	0.3° x 1°	0.9° x 1.25°	(P), N, Fe, Si		z 60 levels	BEC	Moore et al., 2004
Norwegian Earth System Model, Norway	NorESM1-ME	MICOM 0.5° x 0.9°	2.5° x 1.9°	P, N, Fe, Si	CICE4.1	z 53 levels	HAMOC5	Tjiputra et al., 2013

- Formatted ... [66]
- V2 Changes 2018/3/6 6:53 PM
- Deleted: Séférian et al., 2013
- V2 Changes 2018/3/6 6:53 PM
- Formatted ... [67]
- V2 Changes 2018/3/6 6:53 PM
- Formatted ... [70]
- V2 Changes 2018/3/6 6:53 PM
- Formatted ... [68]
- V2 Changes 2018/3/6 6:53 PM
- Formatted ... [69]
- V2 Changes 2018/3/6 6:53 PM
- Deleted: Ilyina et al., 2013
- V2 Changes 2018/3/6 6:53 PM
- Formatted ... [71]
- V2 Changes 2018/3/6 6:53 PM
- Formatted ... [72]
- V2 Changes 2018/3/6 6:53 PM
- Formatted ... [76]
- V2 Changes 2018/3/6 6:53 PM
- Deleted: 4°
- V2 Changes 2018/3/6 6:53 PM
- Formatted ... [73]
- V2 Changes 2018/3/6 6:53 PM
- Formatted ... [74]
- V2 Changes 2018/3/6 6:53 PM
- Formatted ... [75]
- V2 Changes 2018/3/6 6:53 PM
- Formatted ... [77]
- V2 Changes 2018/3/6 6:53 PM
- Formatted ... [78]
- V2 Changes 2018/3/6 6:53 PM
- Formatted ... [79]
- V2 Changes 2018/3/6 6:53 PM
- Formatted ... [81]
- V2 Changes 2018/3/6 6:53 PM
- Deleted: Moore et al., 2004
- V2 Changes 2018/3/6 6:53 PM
- Formatted ... [80]
- V2 Changes 2018/3/6 6:53 PM
- Formatted ... [82]
- V2 Changes 2018/3/6 6:53 PM
- Formatted ... [83]
- V2 Changes 2018/3/6 6:53 PM
- Formatted ... [86]
- V2 Changes 2018/3/6 6:53 PM
- Deleted: Tjiputra et al., 2013
- V2 Changes 2018/3/6 6:53 PM
- Formatted ... [84]
- V2 Changes 2018/3/6 6:53 PM
- Formatted ... [85]
- V2 Changes 2018/3/6 6:53 PM
- Deleted: Geophysical Fluid Dynam...
- V2 Changes 2018/3/6 6:53 PM
- Formatted ... [87]
- V2 Changes 2018/3/6 6:53 PM
- Formatted ... [88]
- V2 Changes 2018/3/6 6:53 PM
- Formatted ... [89]
- V2 Changes 2018/3/6 6:53 PM
- Formatted ... [90]
- V2 Changes 2018/3/6 6:53 PM
- Deleted: .
- V2 Changes 2018/3/6 6:53 PM
- Formatted ... [91]
- V2 Changes 2018/3/6 6:53 PM
- Formatted ... [92]
- V2 Changes 2018/3/6 6:53 PM
- Formatted ... [64]
- V2 Changes 2018/3/6 6:53 PM
- Formatted ... [65]

2.3 Sea-Air CO₂ Flux Drivers: The Seasonal Cycle Diagnostic Framework

The seasonal cycle diagnostic framework was developed as a way of scaling the rates of change of SST and the total DIC driven changes to the seasonal cycle of pCO₂ on a common DIC scale (Mongwe et al., 2016). We use the framework to explore how understanding differences emerging from the temperature and DIC driven CO₂ variability could be helpful as a diagnostic of the apparent observations –model seasonal cycle biases in the Southern Ocean.

The total rate of change of DIC in the surface layer consists of the contribution of air-sea exchanges, biological, vertical and horizontal transport-driven changes (Eq. 1).

$$\left(\frac{\partial DIC}{\partial t}\right)_{Tot} = \left(\frac{\partial DIC}{\partial t}\right)_{air-sea} + \left(\frac{\partial DIC}{\partial t}\right)_{Bio} + \left(\frac{\partial DIC}{\partial t}\right)_{Vert} + \left(\frac{\partial DIC}{\partial t}\right)_{Hor} \quad (1)$$

Because we used zonal means from medium resolution models, we assume that the horizontal terms are negligible, which leaves air-sea exchange, vertical fluxes (advection and diffusion) and biological processes as the dominant drivers of DIC. In order to constrain the contribution of temperature on the seasonal variability of pCO₂ and fCO₂ we derived a new “DIC equivalent term” (DIC_T) defined as the magnitude of DIC change that would correspond to a change in pCO₂ driven by a particular temperature change. In this way the ΔpCO₂, driven solely by modelled or observed temperature change, is converted into equivalent DIC units, which allows its contribution to be scaled against the observed or modelled total surface DIC change (Eq.1).

441 [This calculation of \$DIC_T\$ is done in two steps: firstly, the temperature impact on \$pCO_2\$ is calculated using the](#)
442 [Takahashi et al., \(1993\) empirical expression that linearizes the temperature dependence of the equilibrium](#)
443 [constants.](#)

$$444 \left(\frac{\partial pCO_2}{\partial t} \right)_{SST} = 0.0423 \times pCO_2 \times \left(\frac{\partial pCO_2}{\partial SST} \right) \quad (2)$$

445 [Though this relationship between \$dSST\$ and \$dpCO_2\$ is based on a linear assumption \(Takahashi et al., 1993\),](#)
446 [this formulation has been shown to hold and has been widely used in literature \(e.g. Bakker et al., 2014;](#)
447 [Feely et al., 2004; Marinov and Gnanadesikan, 2011; Takahashi et al., 2002; Wanninkhof et al., 2010;](#)
448 [Landschützer et al., 2018\). We show in the supplementary material that the extension of this expression](#)
449 [into polar temperature ranges \(\$SST < 2^\circ C\$ \) only introduces a minor additional uncertainty of 4 -5% \(SM Fig.](#)
450 [S4\)](#)

451 [Secondly, the temperature driven change in \$pCO_2\$ is converted to an equivalent \$DIC_T\$ using the Revelle](#)
452 [factor.](#)

$$453 \left(\frac{\partial DIC_T}{\partial t} \right)_{SST} = \frac{DIC}{\gamma_{DIC} \times pCO_2} \left(\frac{\partial pCO_2}{\partial t} \right)_{SST} \quad (3)$$

454 [Here we also used a fixed value for the Revelle Factor \(\$\gamma_{DIC}=14\$ \), typical of polar waters the Southern Ocean](#)
455 [but in order to assess the error linked to this assumption. We recomputed the Revelle factor in the Sub-](#)
456 [Antarctic and Antarctic zones using annual mean climatologies of TALK, salinity, sea surface surface](#)
457 [temperature and nutrients. Firstly we examined DIC changes for the nominal range of \$pCO_2\$ change \(340 –](#)
458 [399 \$\mu atm\$:1 \$\mu atm\$ intervals\) and then used this dataset to derive the Revelle factor. The range of calculated](#)
459 [Revelle factors in the Southern Ocean was between \$\gamma_{DIC} \sim 12 - 15.5\$ with an average of \$\gamma_{DIC} = 13.9 \pm 1.3\$. This](#)
460 [justifies our use of \$\gamma_{DIC} = 14\$ for the conversion of the solubility driven \$pCO_2\$ change to an equivalent DIC](#)
461 [\(DICT\) throughout the analysis. We have provided the uncertainty that this conversion makes into the](#)
462 [temperature constraint \$DIC_T\$, by using the upper and lower limits of the Revelle factor \(\$\gamma_{DIC} = 12 - 15.5\$ \) in](#)
463 [the model framework. In the Supplementary Material \(Fig. S5\) we show an examples for observations in](#)
464 [the Sub-Antarctic and Antarctic zones, which show that the extremes of the Revelle factor values \(\$\gamma_{DIC} = 12\$](#)
465 [– \$15.5\$ \) do not alter the phasing or magnitude of the relative controls of temperature or DIC on the seasonal](#)
466 [cycle of \$pCO_2\$.](#)

467 [The rate of change of DIC was discretized on a monthly mean as follows:](#)

468

V2 Changes 2018/3/6 6:53 PM

Formatted: normal, Right, Tabs: 7,62 cm, Centered + 15,24 cm, Right, Position:Horizontal: Left, Relative to: Column, Vertical: In line, Relative to: Margin, Wrap Around

V2 Changes 2018/3/6 6:53 PM

Formatted: Default Paragraph Font

469
$$\left(\frac{\partial DIC_T}{\partial t}\right)_{SST} \approx \left(\frac{\Delta DIC}{\Delta t}\right)_{n,l} = \frac{DIC_{n+1,l} - DIC_{n,l}}{1 \text{ month}} \quad (4)$$

470
 471 Where n is time in month, l is vertical level (in this case the surface, $l=1$). We here take the forward
 472 derivative such that November rate is the difference between December the 15th and November the 15th,
 473 thus being centered at the interval between the months.

474 Finally, to characterize periods of temperature or DIC dominance as main drivers of the instantaneous
 475 (monthly) pCO_2 change we subtract Eq. 4 from Eq. 1, which yields a residual indicator M_{T-DIC} Eq. 5. M_{T-DIC} is
 476 then used as indicator of the dominant driver of instantaneous pCO_2 changes, in this scale monthly time
 477 scale.

479
$$M_{T-DIC} = \left| \left(\frac{\partial DIC_T}{\partial t}\right)_{SST} \right| - \left| \left(\frac{\partial DIC}{\partial t}\right)_{Tot} \right| \quad (5)$$

480
 481 $M_{T-DIC} > 0$ indicates that the pCO_2 variability is dominated by the temperature driven solubility and when
 482 $M_{T-DIC} < 0$, it indicates that pCO_2 changes are mainly modulated by DIC processes (i.e. Biological CO_2 changes
 483 and vertical scale physical DIC mechanisms). We also the following DIC processes; i.) Biological DIC changes
 484 using chlorophyll, NPP, export carbon, surface oxygen, and ii.) . Physical DIC mechanisms using estimated
 485 entrainment rates at the base of the mixed layer: details of this calculation are in section 2.4.

486 In the Southern Ocean, salinity and TALK are considered lower order drivers of the seasonal cycle of pCO_2
 487 (Takahashi et al., 1993). In the supplementary material (Fig. S6), we show that salinity and TALK do not play
 488 a major role as drivers of the local seasonal cycle of pCO_2 . We do so by computing the equivalent rate of
 489 change of DIC resulting from seasonal variability of salinity and TALK as done for temperature (Eq. 2), i.e.
 490 still assuming empirical linear relationships from Takahashi et al (1993): $\left(\frac{\ln(pCO_2)}{\ln(TALK)}\right) \approx -9.4$ and $\left(\frac{\ln(pCO_2)}{\ln(Sal)}\right) =$
 491 0.94). By applying these relationships to the model data, we confirmed that indeed salinity and TALK are
 492 secondary drivers of pCO_2 changes i.e. $\left[\left(\frac{\partial DIC}{\partial t}\right)_{Tot}\right]_{average} \approx 5 \mu\text{mol kg}^{-1} \text{ month}^{-1}$, while $\left[\left(\frac{\partial DIC}{\partial t}\right)_{Tot}\right]_{average}$
 493 $\approx 0.6 \mu\text{mol kg}^{-1} \text{ month}^{-1}$ and $\left[\left(\frac{\partial DIC}{\partial t}\right)_{TALK}\right]_{maximum} \approx 0.4 \mu\text{mol kg}^{-1} \text{ month}^{-1}$.

494 The seasonal cycle of the ocean-atmosphere pCO_2 gradient (ΔpCO_2) is the main driver of the variability of
 495 FCO_2 over comparable periods (Sarmiento and Gruber, 2006; Wanninkhof et al., 2009; Mongwe et al.,
 496 2016). Wind speed plays a dual role as a driver of FCO_2 : it drives the seasonal evolution of buoyancy-
 497 mixing dynamics, which influences the biogeochemistry and upper water column physics but these

V2 Changes 2018/3/6 6:53 PM
Formatted: normal, Space After: 12 pt, No widow/orphan control

V2 Changes 2018/3/6 6:53 PM
Moved (insertion) [2]

V2 Changes 2018/3/6 6:53 PM
Deleted: ocean-atmosphere CO_2 gradient (ΔpCO_2) is known to be the main driver of FCO_2 variability (Sarmiento and Gruber, 2006; Wanninkhof et al., 2009). For this analysis we consider that atmospheric CO_2 is relatively uniform in the Southern Ocean (Fujita et al., 2003), therefore changes in surface ocean pCO_2 mostly drive FCO_2 . Surface ocean pCO_2 is controlled by two key factors; temperature through solubility and DIC concentration through mixing and biological processes (Hauck et al., 2015; Le Quéré and Saltzman, 2013). We use this conjecture as a basis to explore the drivers of the FCO_2 seasonal cycle as applied in Mongwe et al., (2016). ... [93]

V2 Changes 2018/3/6 6:53 PM
Formatted: normal, Right, Tabs: 7,62 cm, Centered + 15,24 cm, Right, Position:Horizontal: Left, Relative to: Column, Vertical: In line, Relative to: Margin, Wrap Around

V2 Changes 2018/3/6 6:53 PM
Formatted: Default Paragraph Font

514 [processes are incorporated into the variability of the DIC. Wind speed also drives the rate of gas exchange](#)
 515 [across the air - seas interface \(Wanninkof et al., 2013\) however, because winds in the Southern Ocean do](#)
 516 [not have large seasonal variation \(Young, 1999\), for this analysis we neglect the role of wind as secondary](#)
 517 [driver of the seasonal cycle of FCO₂. Consequently, the seasonal cycle of FCO₂ is directly linked to surface](#)
 518 [pCO₂ are driven by changes in temperature, salinity, TALK and DIC \(Sarmiento and Gruber, 2006;](#)
 519 [Wanninkhof et al., 2009\). In this analysis we use this assumption as a basis to explore how the seasonal](#)
 520 [variability of temperature and DIC regulate the seasonal cycle of pCO₂ in CMIP5 models relative to](#)
 521 [observational product estimates.](#)

524 2.4 Entrainment mixing

526 [CO₂ uptake by the Southern Ocean has been shown to weaken during winter in the Southern Ocean linked](#)
 527 [to the entrainment of sub-surface DIC as the MLD deepens \(e.g. Lenton et al., 2013; Metzl et al., 2006;](#)
 528 [Takahashi et al., 2009\). Here we estimate this rate of entrainment \(RE\) using Eq. 6, which estimate the](#)
 529 [advection of preformed DIC at the base of the mixed layer:](#)

$$531 RE = U_e \left(\frac{\partial DIC}{\partial z} \right)_{MLD} \quad (6)$$

$$532 RE_n = \left(\frac{\Delta MLD_n}{\Delta t} \right) \left(\frac{\Delta DIC}{\Delta z} \right)_{n,MLD} \quad (7)$$

$$533 \left(\frac{\Delta DIC}{\Delta z} \right)_{n,MLD} = \frac{DIC_{n,MLD_{n+1}} - DIC_{n,MLD_n}}{\Delta z} \quad (8)$$

534
 535 [In which U_e is an equivalent entrainment velocity based on the rate of change of the MLD. This](#)
 536 [approximation of vertical entrainment is necessary as it is not possible to compute this term from the](#)
 537 [CMIP5 data because the vertical DIC distribution is only available as annual means. We use the entrainment](#)
 538 [rates to estimates the influence of subsurface/bottom DIC changes on surface DIC changes driven and](#)
 539 [subsequently pCO₂ and FCO₂. Because we are mainly interested in the period autumn – winter, where the](#)
 540 [MLD ≥ 60 m in the Sub-Antarctic zone and ≥ 40 m in the Antarctic zone, at this depth seasonal variations in](#)
 541 [DIC are anticipated to be minimal thus these estimates can be used. The monthly and annual mean DIC](#)
 542 [from a NEMO PISCES 0.5 x 0.5o model output was used to estimate the uncertainty by comparing RE](#)
 543 [computed from both \(Dufour et al., 2013\). We found that the annual and monthly estimates to be indeed](#)
 544 [comparable with minimal differences \(not shown\). It is noted as a caveat that this rate of entrainment is](#)
 545 [only a coarse estimate because we were using annual means, and is intended only for the autumn-winter](#)
 546 [period when MLDs are deepen.](#)

V2 Changes 2018/3/6 6:53 PM

Formatted: normal, Adjust space between Latin and Asian text, Adjust space between Asian text and numbers

V2 Changes 2018/3/6 6:53 PM

Deleted: Fluxes

V2 Changes 2018/3/6 6:53 PM

Formatted: normal

V2 Changes 2018/3/6 6:53 PM

Deleted: CO₂ uptake has been shown to weaken during the winter season in the Southern Ocean linked to the entrainment of sub-surface DIC due to MLD changes (e.g. Lenton et al., 2013; Metzl et al., 2006; Takahashi et al., 2009). DIC entrainment fluxes (F_{DIC}) at the base of the mixed layer were estimated as follow: - [... \[94\]](#)

V2 Changes 2018/3/6 6:53 PM

Formatted: normal, Right, Tabs: 7,62 cm, Centered + 15,24 cm, Right, Position: Horizontal: Left, Relative to: Column, Vertical: In line, Relative to: Margin, Wrap Around

V2 Changes 2018/3/6 6:53 PM

Formatted: Default Paragraph Font

557
558
559
560
561
562
563
564
565
566
567
568
569
570
571
572
573
574
575
576
577
578
579
580
581
582
583
584
585
586
587
588
589

3. Results

3.1 Annual climatological sea-air CO₂ fluxes

The annual mean climatological distribution of FCO₂ in the Southern Ocean [obtained from observational products](#) is spatially variable but mainly characterized by two key features: (i) CO₂ in-gassing north of 50°-55°S (Polar Frontal zone, PFZ) within and north of the Sub-Antarctic Zone, and (ii), CO₂ out-gassing between the [PF \(~ 58°S\)](#) and the Marginal Ice Zone (MIZ, [~ 60° - 68°S](#)) (Fig. 1a-b). [Most](#) CMIP5 models broadly capture these features, however, they also show significant differences in space and magnitude between the basins of the Southern Ocean (Fig. 1). With the exception of CMCC-CESM, which shows a northerly-extended CO₂ outgassing band between about 40°S and 50°S, CMIP5 models generally show the CO₂ outgassing zone between 50°S – 70°S [in agreement](#) with observational estimates (Fig. 1).

[The analyzed 10 CMIP5 models show a large spatial dispersion in the spatial representation of the magnitudes of FCO₂ with respect to observations \(Fig. 1, Table 2\). They generally overestimate the upwelling-driven CO₂ outgassing \(55°S -70°S\) in some basins relative to observations. IPSL-CM5A, CanESM2, MPI-ESM, GFDL-ESM2M and MRI-ESM, for example, show CO₂ outgassing fluxes reaching up to 25 g m⁻² yr⁻¹, while observations only show a maximum of 8 g m⁻² yr⁻¹ \(Fig. 1\). Between 40°S - 56°S \(Sub-Antarctic zone\), observations and CMIP5 models largely agree, showing a CO₂ in-gassing feature, which is mainly attributable to biological processes \(McNeil et al., 2007; Takahashi et al., 2012\). South of 65°S, in the MIZ, models generally show an excessive CO₂ ingassing with respect to observations \(with the exception of CanESM2, IPSL-CM5A-MR and CNRM-CM5\). Note that as much as this bias south of the MIZ might be a true divergence of CMIP5 models from the observed ocean, it is also possibly due to the lack of observations in this region, especially during the winter season \(Bakker et al., 2014; Monteiro, 2010\).](#)

[Table 2 shows the](#) Pattern Correlation Coefficient (PCC) and the Root Mean Square Error (RMSE), [which are](#) here used to quantify the model [spatial and magnitude](#) performances [against Landschützer et al \(2014\) data product](#). Out of the 10 models, 6 show a moderate spatial correlation with [Landschützer et al \(2014\)](#) (PCC = 0.40 – 0.60), i.e. CNRM-CM5, GFDL-ESM2M, HadGEM2-ES, IPSL-CM5A-MR, CESM1-BGC, [NorESM-ME](#) and CanESM2. While MPI-ESM-MR (PCC = 0.37), MRI-ESM (PCC = 0.36) and CMCC-CESM (PCC = -0.09) show a weak to null spatial correlation with observations, the latter mainly due to the overestimated outgassing region. [Spatially, GFDL-ESM2M and NorESM1-ME are the most comparable to Landschützer et al](#)

V2 Changes 2018/3/6 6:53 PM
Moved up [2]:)

V2 Changes 2018/3/6 6:53 PM
Deleted: T is time in months and DIC_{sub} is the subsurface DIC concentration at the base of the MLD. Annual mean DIC were used here mainly because vertical DIC fields are only available in annual means at the CMIP5 portal and observations (GLODAP). However because we are mainly interested in the period autumn – winter, where the MLD ≥ 60 m in the Sub-Antarctic zone and ≥ 40 m in the Antarctic zone (Fig 6a-f), DIC seasonality is anticipated to be minimal at this depth. To evaluate the uncertainty of using annual means, we assessed DIC entrainment fluxes using a model simulation at 0.5 degrees resolution (Dufour et al., 2013) with annual and monthly mean outputs. It was found that the estimates are indeed comparable with minimal differences (not shown). It is ... [97]

V2 Changes 2018/3/6 6:53 PM
Formatted ... [96]

V2 Changes 2018/3/6 6:53 PM
Formatted: Font:11 pt

V2 Changes 2018/3/6 6:53 PM
Formatted: normal

V2 Changes 2018/3/6 6:53 PM
Deleted: The Southern Ocean is her ... [98]

V2 Changes 2018/3/6 6:53 PM
Moved up [1]: Within the Sub-Ant ... [99]

V2 Changes 2018/3/6 6:53 PM
Deleted: PFZ

V2 Changes 2018/3/6 6:53 PM
Deleted: The

V2 Changes 2018/3/6 6:53 PM
Deleted: , agreeing

V2 Changes 2018/3/6 6:53 PM
Deleted: The analyzed CMIP5 moc ... [100]

V2 Changes 2018/3/6 6:53 PM
Formatted: normal

V2 Changes 2018/3/6 6:53 PM
Deleted:) presented in Table 2 have been

V2 Changes 2018/3/6 6:53 PM
Deleted: .

V2 Changes 2018/3/6 6:53 PM
Deleted: observations

V2 Changes 2018/3/6 6:53 PM
Deleted: ~

V2 Changes 2018/3/6 6:53 PM
Deleted: NorESM2

V2 Changes 2018/3/6 6:53 PM
Formatted ... [95]

V2 Changes 2018/3/6 6:53 PM
Formatted: Default Paragraph Font

683 [\(2014\)](#), (RMSE < 9), while CCMC-CESM, CanESM2, MRI-ESM and CNRM-CM5 shows the most differences
684 [\(RMSE > 15\)](#). The rest of the models show a modest comparison (RMSE 9 – 11).
685
686 [NorESM1-ME](#) and CESM1-BGC are [the only 2](#) of the [10](#) models showing [a consistent](#) spatial (RMSE < 10)
687 and magnitude ([PCC = 0.50](#)) performance. From Table 2, it is evident that an appropriate representation of
688 the spatial properties of FCO₂ with respect to observations does not always correspond [to comparable](#)
689 magnitudes. CanESM2 for example shows a good spatial comparison (PCC = 0.54), yet [a](#) poor estimation of
690 the magnitudes (RMSE = 19.5). [In this case](#) caused by an overestimation of CO₂ uptake north of 55°S (≈ - 28
691 g m⁻² yr⁻¹) and CO₂ outgassing (> 25 g m⁻² yr⁻¹) in the Antarctic zone, resulting in a net [total](#) Southern Ocean
692 annual weak sink (-0.05 Pg C m⁻² yr⁻¹). [These inconsistencies in the spatial and magnitude performances](#)
693 highlights [some of](#) the limitations of using annual mean indicators to evaluate model performance and [thus](#)
694 [a](#) process-based diagnostic approach [could be useful in understanding the departure of models from](#)
695 [observed estimates](#).

697 3.2 Sea-Air CO₂ Flux Seasonal Cycle Variability and Biases

698
699 The seasonal cycle of FCO₂ is shown in Fig. 2. [The seasonality of FCO₂ in the 10 CMIP5 models shows a large](#)
700 [dispersion in both phasing and amplitude, but mostly disagree with observations in the phase of the](#)
701 [seasonal cycle as well as with each other. More quantitatively, CMIP5 models show weak to negative](#)
702 [correlations with the Landschützer et al \(2014\) data product in the Sub-Antarctic Zone and have slightly](#)
703 [higher correlations in the Antarctic Zone \(see supplementary Fig. S7\). This discrepancy is consistent with](#)
704 [Anav et al., \(2013\) findings, who however used fixed latitude criteria. Based on the phasing, the seasonality](#)
705 [of FCO₂ in CMIP5 models can be a priori divided in two main groups: group-DIC models, comprising of MPI-](#)
706 [ESM, HadGEM-ES and NorESM1-ME, and group-SST models, the remainder i.e. GFDL-ESM2M, CMCC-CESM,](#)
707 [CNRM-CERFACS, IPSL-CM5A-MR, CESM1-BGC, MRI-ESM and CanESM2. The naming convention is](#)
708 [suggestive of the mechanism driving the seasonal cycle, as it will be clarified further on. A similar grouping](#)
709 [was also identified by Kessler and Tjiputra \(2016\) using a different criterion. \[Fig. 3\]\(#\) shows the seasonal cycle](#)
710 [of FCO₂ of an equally-weighted ensemble of the two groups compared to observations, the shaded area](#)
711 [shows the decadal standard deviation for the models and the Landschützer et al \(2014\) data product for](#)
712 [1998 -2014 standard deviation for in the various regions.](#)

714 In the Sub-Antarctic zone, [the observational products](#) show a weakening of CO₂ uptake during winter (less
715 negative values in [June-August](#)) with values close to the zero [at the onset of spring \(September\)](#) in all three
716 [basins](#). Similarly, during the spring season, all three basins are seen to maintain a steady increase of CO₂

- V2 Changes 2018/3/6 6:53 PM
Deleted: NorESM2
- V2 Changes 2018/3/6 6:53 PM
Deleted: two
- V2 Changes 2018/3/6 6:53 PM
Deleted: ten
- V2 Changes 2018/3/6 6:53 PM
Deleted: the best performance in both
- V2 Changes 2018/3/6 6:53 PM
Deleted: PCC > 0.50
- V2 Changes 2018/3/6 6:53 PM
Deleted: RSME < 10) indicators
- V2 Changes 2018/3/6 6:53 PM
Deleted: in respect of
- V2 Changes 2018/3/6 6:53 PM
Deleted: with
- V2 Changes 2018/3/6 6:53 PM
Deleted: This is thought to be
- V2 Changes 2018/3/6 6:53 PM
Deleted: This outcome
- V2 Changes 2018/3/6 6:53 PM
Deleted: highlights the need for a more
- Moved (insertion) [3]
- V2 Changes 2018/3/6 6:53 PM
Deleted: CMIP5 models are generally out of phase with observations as well as with each other (e.g. Anav et al., 2013). Based on the phase, the seasonality of FCO₂ in CMIP5 models can be a priori divided in two main groups: group A comprising of MPI-ESM, HadGEM-ES and NorESM, and group B, the remainder i.e. GFDL-ESM2M, CMCC-CESM, CNRM-CERFACS, IPSL-CM5A-MR, CESM1-BGC, NorESM2, MRI-ESM and CanESM2. A similar grouping was first identified by Kessler and Tjiputra, 2016. Fig. 3 presents the ensemble seasonal cycle of FCO₂ for these two groups compared to observations, with the ... [102]
- V2 Changes 2018/3/6 6:53 PM
Formatted: normal
- V2 Changes 2018/3/6 6:53 PM
Deleted: for all three basins, observed FCO₂
- V2 Changes 2018/3/6 6:53 PM
Deleted: JJA
- V2 Changes 2018/3/6 6:53 PM
Deleted: flux
- V2 Changes 2018/3/6 6:53 PM
Deleted: .
- V2 Changes 2018/3/6 6:53 PM
Formatted ... [101]
- V2 Changes 2018/3/6 6:53 PM
Formatted: Default Paragraph Font

762 uptake until mid-summer (December), while they differ during autumn (March-May). The Pacific Ocean
763 shows an increase in CO₂ uptake during autumn that is not observed in the other basins (only marginally in
764 the Indian Ocean). In the Antarctic zone, the observed FCO₂ seasonal cycle is mostly similar in all three
765 basins (Fig. 3d-f). While this seasonal cycle consistency may suggest a spatial uniformity of the mechanisms
766 of FCO₂ at the Antarctic, we are also mindful that this may be due to a result of the paucity of observations
767 in this area. In the Antarctic zone, all three basins show a weakening of CO₂ uptake from the onset of
768 autumn (March) until mid-winter (June-July) when it outgasses. The winter CO₂ outgassing is followed by a
769 strengthening of the CO₂ uptake throughout spring to summer, when it reaches a CO₂ ingassing peak.

V2 Changes 2018/3/6 6:53 PM
Deleted: MAM...arch-May). The Pa ... [103]

771 The differences in the seasonal cycle of FCO₂ across the three basins of the Sub-Antarctic zone found in the
772 observational product (Fig. 2), likely resemble the differences in the spatial behavior seen in Fig. 1. To verify
773 this, we correlate the seasonal cycles from the Landschützer et al (2014) observational product in the three
774 basins (Fig. 4). The FCO₂ seasonal cycle in the Sub-Antarctic Atlantic and Indian basins is the only one that is
775 similar (R = 0.8), while the other basins are quite different to each other (R = -0.1 for Pacific – Atlantic and
776 R ~ 0.4 for Pacific – Indian). Contrary to the observational product, CMIP5 models show the same seasonal
777 cycle phasing across all three basins in the Sub-Antarctic zone (basin – basin correlation coefficients are
778 always larger than 0.50 in Fig. 4), with the exception of three models (i.e. CMCC-CESM, CESM-BGC1 and
779 GFDL-ESM2M). In the Antarctic zone, CMIP5 models agree with observations in the spatial uniformity of the
780 seasonal cycle of FCO₂ among the three basins.

V2 Changes 2018/3/6 6:53 PM
Deleted: simulated ...ifferences in ... [104]

782 Group₂DIC models are characterized by an exaggerated CO₂ uptake during spring-summer (Fig. 3) with
783 respect to observations estimates and CO₂ outgassing during winter. These models generally agree with
784 observations in the phasing of CO₂ uptake during spring, but overestimate the magnitudes. It is worth
785 noting that the seasonal characteristics of group₂DIC models are mostly in agreement with the observations
786 in the Atlantic and Indian basin in Sub-Antarctic zone (R > 0.5 in Fig. 4). The large standard deviation (~ 0.01
787 g C m⁻² day⁻¹) during the winter and spring-summer seasons in the Atlantic Ocean shows that though group-
788 DIC models agree in the phase, magnitudes vary considerably (Fig. 3b). For example MPI-ESM reach up to
789 0.06 g C m⁻² day⁻¹ outgassing during winter, while HadESM2-ES and NorESM2 peak only at ~ 0.03 g C m⁻²
790 day⁻¹. Group-SST models on the other hand are characterized by a CO₂ outgassing peak in summer (Dec-
791 Feb) and a CO₂ in-gassing peak at the end of autumn (May) and their phase is opposite to the observational
792 estimates in the Atlantic and Indian basins (Fig. 3b,c). Group-SST models only show a strengthening of CO₂
793 uptake during spring in the Indian Ocean. Interestingly, group-SST models compare relatively well with the
794 observed FCO₂ seasonal cycle in the Pacific Ocean, whereas group₂DIC models disagree the most with the
795 observed estimates (Fig. 3a). This phasing differences within models and against observed estimates

V2 Changes 2018/3/6 6:53 PM
Formatted: normal

V2 Changes 2018/3/6 6:53 PM
Deleted: A ensemble...DIC models ... [105]

V2 Changes 2018/3/6 6:53 PM
Formatted: normal, Right, Tabs: 7,62 cm, Centered + 15,24 cm, Right, Position:Horizontal: Left, Relative to: Column, Vertical: In line, Relative to: Margin, Wrap Around

V2 Changes 2018/3/6 6:53 PM
Formatted: Default Paragraph Font

844 probably suggests that the disagreement of CMIP5 models FCO_2 with observations is not a matter of a
 845 relative error/constant magnitude offset, but likely point to differences in the seasonal drivers of FCO_2 .
 846
 847 In the Antarctic zone (Fig. 3d-f), both group-DIC and group-SST models perform better than the Sub-
 848 Antarctic, also in more quantitative terms as shown by the correlation analysis in Fig. S7. However, the
 849 similarity in the seasonality of the different basins found in the observational product is now properly
 850 simulated by the models (Fig. 4, with the exception of MRI-ESM and CanESM2 where $R < 0$ for all three
 851 basins). Here FCO_2 magnitudes oscillate around zero with the largest disagreements occurring during mid-
 852 summer, where observations estimates shows a weak CO_2 sink ($\approx -0.03 \text{ gC m}^{-2} \text{ day}^{-1}$), group-SST showing a
 853 zero net CO_2 flux and a strong uptake in group-DIC shows (e.g. $\approx -0.12 \text{ gC m}^{-2} \text{ day}^{-1}$ in the Pacific Ocean). The
 854 large standard deviation ($\approx 0.01 \text{ gC m}^{-2} \text{ day}^{-1}$) here indicates considerable differences among models (Fig.
 855 3d-f).

- V2 Changes 2018/3/6 6:53 PM
Deleted: ... (Fig. 3d-f), both group ... [107]
- V2 Changes 2018/3/6 6:53 PM
Moved down [4]: 3d-f.
- V2 Changes 2018/3/6 6:53 PM
Deleted: The values ...oscillate arou ... [108]
- V2 Changes 2018/3/6 6:53 PM
Moved up [3]: Fig.
- V2 Changes 2018/3/6 6:53 PM
Deleted: 2d-f). - ... [109]
- V2 Changes 2018/3/6 6:53 PM
Moved (insertion) [4]
- V2 Changes 2018/3/6 6:53 PM
Deleted: overestimation or underestimation irrespective of the sign of the flux. For each basin, the models were ranked according to their mean annual bias. Fig. 4 clearly shows that CMIP5 models have a general positive bias against observations during summer and/or autumn with the exception of group-A models in the Sub-Antarctic zone. W ... [110]
- V2 Changes 2018/3/6 6:53 PM
Deleted: [111]
- V2 Changes 2018/3/6 6:53 PM
Deleted: the two major drivers (i.e ... [112]
- V2 Changes 2018/3/6 6:53 PM
Formatted: Font:11 pt
- V2 Changes 2018/3/6 6:53 PM
Deleted: ($\frac{\Delta SST}{\Delta t} > 0$) occurring in th ... [113]
- V2 Changes 2018/3/6 6:53 PM
Formatted: Font:12 pt
- V2 Changes 2018/3/6 6:53 PM
Deleted: $\frac{\Delta SST}{\Delta t}$ dSST/dt...have import ... [114]
- V2 Changes 2018/3/6 6:53 PM
Deleted: The computed $\frac{\Delta SST}{\Delta t}$
- V2 Changes 2018/3/6 6:53 PM
Formatted: Font:11 pt
- V2 Changes 2018/3/6 6:53 PM
Deleted: Fig. 5
- V2 Changes 2018/3/6 6:53 PM
Formatted: Font:12 pt
- V2 Changes 2018/3/6 6:53 PM
Deleted: temperature variability... [115]
- V2 Changes 2018/3/6 6:53 PM
Formatted: Not Superscript/ Subscript
- V2 Changes 2018/3/6 6:53 PM
Deleted: > 0 (red) indicates period ... [116]
- V2 Changes 2018/3/6 6:53 PM
Formatted
- V2 Changes 2018/3/6 6:53 PM
Formatted: Default Paragraph Font

857 **3.3 Seasonal Scale Drivers of Sea-Air CO_2 Flux**

858
 859 We now examine how changes in temperature and DIC regulate FCO_2 variability at the seasonal scale
 860 following the method described in Sec. 2.3. Fig. 5 shows the monthly rates of change of SST ($dSST/dt$) for
 861 the 10 models compared with WOA13 SST. CMIP5 generally shows agreement in the timing of the switch
 862 from surface cooling ($dSST/dt < 0$) to warming ($dSST/dt > 0$) and vice versa; i.e. March (summer to
 863 autumn), and September (winter to spring) respectively. In both the Sub-Antarctic and Antarctic zone
 864 CMIP5 models agree with observations in this timing (Fig. 5). However, while they agree in phasing, the
 865 amplitude of these warming and cooling rates are overestimated with respect to the WOA13 dataset with
 866 exception of NorESM1-ME. Subsequently these differences in the magnitude of $dSST/dt$ have important
 867 implications for the solubility of CO_2 in seawater; larger magnitudes of $|dSST/dt|$ are likely to enhance the
 868 response of the pCO_2 to temperature through CO_2 solubility changes. For example, because the
 869 observations in the Indian Ocean shows a warming rate of about $0.5^\circ\text{C month}^{-1}$ lower compared to the
 870 other two basins, we expect a relatively weaker role of surface temperature in this basin.

871
 872 As described in sec. 2.3, the computed $dSST/dt$ magnitudes were used to estimate the equivalent rate of
 873 change of DIC driven by CO_2 solubility using Eq. 2. The seasonal cycle of $|dDIC_T/dt|_{SST}$ vs $|dDIC/dt|_{Tot}$ for
 874 the 10 models and observations is presented in the supplementary material (Fig. S8), here we show the
 875 seasonal mean of M_{T-DIC} Eq. 3. As articulated in sec. 2.3, M_{T-DIC} (Fig. 6) is the difference between the total
 876 surface DIC rate of change of DIC (Eq. 1) and the estimated equivalent temperature driven solubility DIC
 877 changes Eq. 3, such that when $|dDIC_T/dt|_{SST} > |dDIC/dt|_{Tot}$, temperature is the dominant driver of the

1012 instantaneous $p\text{CO}_2$ changes, and conversely when $|d\text{DIC}_T/dt|_{\text{SST}} < |d\text{DIC}/dt|_{\text{Tot}}$, DIC processes is the
 1013 dominant mode in the instantaneous $p\text{CO}_2$ variability. The models showing the former feature are SST-
 1014 driven and belong to group-SST, while the models showing the latter are DIC-driven and belong to group-
 1015 SST.

1016
 1017 According to the $M_{T-\text{DIC}}$ magnitudes in Fig. 6, the seasonal cycle of $p\text{CO}_2$ in the observational estimates is
 1018 predominantly DIC-driven most of the year in both the Sub-Antarctic and Antarctic zone. Note that,
 1019 however, during periods of high $|d\text{SST}/dt|$, i.e. autumn and spring, observations show a moderate to weak
 1020 DIC control ($M_{T-\text{DIC}} \approx 0$). The Antarctic zone is mostly characterized by a stronger DIC control (mean Annual
 1021 $M_{T-\text{DIC}} > 3$) except for the spring season (Fig. 6). Consistent with the similarity analysis presented in Fig. 4,
 1022 the Antarctic zone shows coherence in the sign of the temperature –DIC indicator ($M_{T-\text{DIC}} > 0$) within the
 1023 three basins.

1024
 1025

1026 3.4 Source terms in the DIC surface budget

1027
 1028 To further constrain the surface DIC budget in Eq. 1, we examine the role of the biological source term
 1029 using chlorophyll and Net Primary Production (NPP) as proxies. Fig. 8 shows the seasonal cycle of
 1030 chlorophyll, NPP and the rate of surface DIC changes ($d\text{DIC}/dt$). The observed seasonal cycle of chlorophyll
 1031 (Johnson et al., 2013) shows a similar seasonal cycle within the three basins during the spring – summer
 1032 seasons (autumn-winter data are removed due to the satellite limitation) in both Sub-Antarctic and
 1033 Antarctic zone. Magnitudes are however different in the Sub-Antarctic zone; the Atlantic basin shows larger
 1034 chlorophyll magnitudes (Chlorophyll reach up to 1.0 mg m^{-3}) compared to the Pacific and Indian basins (Chl
 1035 $< 1 \text{ mg m}^{-3}$).

1036
 1037 CMIP5 models here show a clear partition between group-DIC and group-SST models. While they mostly
 1038 maintain the same phase, group-DIC shows larger amplitudes of chlorophyll relative to group-SST and
 1039 observed estimates in the Sub-Antarctic zone. This difference is even clearer in NPP magnitudes, where
 1040 group-DIC models show a maximum of $\text{NPP} > 1 \text{ mmol m}^{-2} \text{ s}^{-1}$ in summer, while group-SST magnitudes shows
 1041 about half of it. Except for CESM1-BGC and CMCC-CESM (and NorESM1-ME for NPP), each CMIP5 model
 1042 generally maintains a similar chlorophyll seasonal cycle (phase and magnitude) in all three basins of the
 1043 Southern Ocean. This is contrary to the observations, which show differences in the magnitude.
 1044 Consistently with the observational product, CESM1-BGC simulates larger amplitude in the Atlantic basin.
 1045 While CMCC-CESM also has this feature, it also shows an overestimated chlorophyll peak in the Indian

- V2 Changes 2018/3/6 6:53 PM
Deleted: driver of
- V2 Changes 2018/3/6 6:53 PM
Deleted: and when
- V2 Changes 2018/3/6 6:53 PM
Deleted: < 0 (blue) DIC drives the variability of $p\text{CO}_2$ [118]
- V2 Changes 2018/3/6 6:53 PM
Deleted: data
- V2 Changes 2018/3/6 6:53 PM
Formatted: normal
- V2 Changes 2018/3/6 6:53 PM
Formatted: Not Superscript/ Subscript
- V2 Changes 2018/3/6 6:53 PM
Deleted: throughout
- V2 Changes 2018/3/6 6:53 PM
Deleted: (Fig. 6).
- V2 Changes 2018/3/6 6:53 PM
Deleted: that
- V2 Changes 2018/3/6 6:53 PM
Deleted: $\frac{\Delta\text{SST}}{\Delta t}$
- V2 Changes 2018/3/6 6:53 PM
Deleted: close to zero) in the Sub-Antarctic zone.
- V2 Changes 2018/3/6 6:53 PM
Deleted: instead
- V2 Changes 2018/3/6 6:53 PM
Deleted: index
- V2 Changes 2018/3/6 6:53 PM
Deleted: [119]
- V2 Changes 2018/3/6 6:53 PM
Deleted: for CMIP5 models justifies our a priori separation between group A and group B in the Sub-Antarctic zone that was based on a visual inspection in section 3.2. It shows group A models (HadGEM-ES, NorESM2 and MPI-ESM) at the bottom of Fig. 6, indicating that these models are mainly DIC driven. All the group -B models are at the top o ... [120]
- V2 Changes 2018/3/6 6:53 PM
Deleted: CMIP5 models. Here CMI ... [121]
- V2 Changes 2018/3/6 6:53 PM
Formatted: normal
- V2 Changes 2018/3/6 6:53 PM
Deleted: Vertical Fluxes
- V2 Changes 2018/3/6 6:53 PM
Formatted: Font:11 pt, Not Bold
- V2 Changes 2018/3/6 6:53 PM
Deleted: At the onset of autumn, s ... [122]
- V2 Changes 2018/3/6 6:53 PM
Formatted: ... [117]
- V2 Changes 2018/3/6 6:53 PM
Formatted: Default Paragraph Font

1102 Ocean. In the Antarctic zone both observations and CMIP5 models generally agree in both phase and
1103 magnitude (except for CanESM2) of the seasonal cycle of chlorophyll in all three basins.
1104
1105 We now examine the influence of the vertical DIC rate in Eq. 1, using estimated entrainment rates (RE, Eq.
1106 5) based on MLD and vertical DIC gradients (see sec. 2.3). Fig. 7 shows the seasonal changes of MLD
1107 compared with the rate from the observational product. CMIP5 models largely agree on the timing of the
1108 onset of MLD deepening (February in the Pacific Ocean, and March for the Atlantic and Indian Ocean) and
1109 shoaling (September) in the Sub-Antarctic zone (with the exception of NorESM1-ME and IPSL-CM5A in the
1110 Pacific Ocean). The Indian Ocean generally shows deeper winter MLD in both observations and CMIP5
1111 models in the Sub-Antarctic zone. Note that while CMIP5 models generally show the observed deeper
1112 MLDs in the Indian Ocean, they show a large variation; for example, the winter maximum depth range from
1113 100 m (CMCC-CESM, Pacific Ocean) to 350 m (CanESM2, Indian Ocean) in the Sub-Antarctic zone. In the
1114 Antarctic zone CMIP5 models are largely in agreement on the timing of the onset of MLD deepening
1115 (February), but also variable in their winter maximum depth. It is worth noting that the observed MLD
1116 seasonal cycle might be biased due to limited in situ observations particularly in the Antarctic zone (de
1117 Boyer Montégut et al., 2004).
1118
1119 The estimated RE values in Fig. 10 show that almost all CMIP5 (with the exception of NorESM1-ME) entrain
1120 subsurface DIC into the mixed layer during autumn–winter in agreement with the observational estimates.
1121 In the Sub-Antarctic zone, the estimates using the observational products show the strongest entrainment
1122 in the Atlantic Ocean in May (RE reaches up to $10 \mu\text{mol kg}^{-1} \text{month}^{-1}$), while it is lower in the other basins. In
1123 the Antarctic zone, observed RE conversely shows stronger entrainment rates in the Pacific and Indian
1124 Ocean ($\text{RE} > 15 \mu\text{mol kg}^{-1} \text{month}^{-1}$) in comparison to the Atlantic basin ($\text{RE} = 11 \mu\text{mol kg}^{-1} \text{month}^{-1}$). CMIP5
1125 models entrainment rates are variable but not showing any particular deficiency when compared with the
1126 observational estimates. Also, the group-DIC and group-SST models show no clear distinction, the major
1127 striking features being the relatively stronger entrainment in MPI-ESM and CanESM2 across the three
1128 basins in the Sub-Antarctic zone in mid to late winter ($\text{RE} = 15 \mu\text{mol kg}^{-1} \text{month}^{-1}$) and the large winter
1129 entrainment in IPSL-CM5A-MR in the Antarctic Pacific Ocean. The supply of DIC to the surface due to vertical
1130 entrainment is therefore generally comparable between model simulations and the available estimate.
1131
1132 However, our RE estimates are estimated at the base of the mixed layer, which is not necessarily a
1133 complete measure of the vertical flux of DIC at the surface. We therefore investigate the annual mean
1134 vertical DIC gradients in Fig. 10 as an indicator of where the surface uptake processes occur. The simulated
1135 CMIP5 profiles are similar to GLODAP2, but some differences arise. In the Sub-Antarctic zone, GLODAP2

V2 Changes 2018/3/6 6:53 PM

Deleted: (Fig. 8). The MLD rate of change is the dominant driver of F_{DIC} variability because the annual vertical profiles of DIC (S3 & S4 supplementary material) show that, in agreement with observations, the simulated DIC vertical gradients weaken below 90 m and are constant for most of the mesopelagic zone in

V2 Changes 2018/3/6 6:53 PM

Deleted: (>100 m in

V2 Changes 2018/3/6 6:53 PM

Deleted:). Following the smaller monthly change in MLD ($\sim 60 \text{ m month}^{-1}$ vs $\sim 35 \text{ m}$

V2 Changes 2018/3/6 6:53 PM

Deleted: (S5 Supplementary), the

V2 Changes 2018/3/6 6:53 PM

Formatted: normal

V2 Changes 2018/3/6 6:53 PM

Deleted: shows comparable smaller DIC entrainment fluxes with respect to the Sub-Antarctic zone (Fig. 8). Note that while the Antarctic zone shows lower DIC entrainment fluxes compared to

V2 Changes 2018/3/6 6:53 PM

Formatted: normal, Right, Tabs: 7,62 cm, Centered + 15,24 cm, Right, Position:Horizontal: Left, Relative to: Column, Vertical: In line, Relative to: Margin, Wrap Around

V2 Changes 2018/3/6 6:53 PM

Formatted: Default Paragraph Font

1153 [shows a shallower surface maximum in the Atlantic basin consistent with higher biomass in this basin \(Fig.](#)
1154 [8\) \(\(dDIC/dz\)_{smax} = 0.55 μmol kg⁻¹ m⁻¹, at 50 m\) compared to the Pacific \(\(dDIC/dz\)_{smax} = 0.60 μmol kg⁻¹ m⁻¹, at](#)
1155 [80 m\) and Indian basin \(\(dDIC/dz\)_{smax} = 0.40 μmol kg⁻¹ m⁻¹, at 80 m\). CMIP5 models generally do not show](#)
1156 [this feature in the Sub-Antarctic zone, except for CESM1-BGC1 \(\(dDIC/dz\)_{smax} = 0.50 μmol kg⁻¹ m⁻¹, at 50 m\).](#)
1157 [Instead, they show the surface maxima at the same depth in all three basins. In the Antarctic zone both](#)
1158 [CMIP5 models and observations shows larger \(dDIC/dz\)_{smax} magnitudes and nearer surface maxima \(with](#)
1159 [the exception of CanESM2 and CESM1-BGC\). This difference in the position and magnitude of the DIC](#)
1160 [maxima between the Sub-Antarctic and Antarctic zone has important implications for surface DIC changes](#)
1161 [and subsequently pCO₂ seasonal variability. Because of the nearer surface DIC maxima in the Antarctic](#)
1162 [zone, surface DIC changes are mostly influenced by these strong near surface vertical gradients than MLD](#)
1163 [changes. This implies that even if the entrainment rates at the base of the MLD are comparable between](#)
1164 [the Sub-Antarctic and the Antarctic, the surface supply of DIC may be larger in the Antarctic zone.](#)

V2 Changes 2018/3/6 6:53 PM
Deleted: it is characterized by higher DIC vertical gradients in the upper 100 m in CMIP5 models (S4 supplementary).

1167 4. Discussion

1168 [Recent studies have highlighted that important differences exist between the seasonal cycle of pCO₂ in](#)
1169 [models and observations in the Southern Ocean \(Lenton et al., 2013; Anav et al., 2015; Mongwe, 2016\).](#)
1170 [Paradoxically, although the models may be in relative agreement for the mean annual flux, they diverge in](#)
1171 [the phasing and magnitude of the seasonal cycle \(Lenton et al., 2013; Anav et al., 2015; Mongwe, 2016\).](#)
1172 [These differences in the seasonal cycle raise questions about the climate sensitivity of the carbon cycle in](#)
1173 [these models because they may reflect differences in the process sensitivities to drivers that are](#)
1174 [themselves climate sensitive.](#)

V2 Changes 2018/3/6 6:53 PM
Formatted: Font:14 pt, Bold

V2 Changes 2018/3/6 6:53 PM
Formatted: normal

V2 Changes 2018/3/6 6:53 PM
Formatted: Font:16 pt

V2 Changes 2018/3/6 6:53 PM
Formatted: normal, Tabs: 10,75 cm, Left

V2 Changes 2018/3/6 6:53 PM
Formatted: Font:11 pt

V2 Changes 2018/3/6 6:53 PM
Deleted: In this study, we use a diagnostic approach from Mongwe et al., 2016 as a basis to investigate processes regulating FCO₂ at the seasonal scale in earth system models, assessing the behaviour of 10 CMIP5 ESMs against available observations in the Southern Ocean. The 10 models analyzed can be divided in two major groups (Fig. 3): Group A consisted of models that overestimate the role of the DIC as the main driver of pCO₂ (hence FCO₂), and Group B, which overestimates the role of temperature in FCO₂ seasonal variability. These two classes of CMIP5 models were first distinguished by Kessler and Tjiputra (2016). Kessler and Triputra (2016) describe how FCO₂ seasonal biases in these two groups predispose equivalent biases in the long term CO₂ projections, where, for example, models which overestimate biological CO₂ uptake result in a stronger century scale CO₂ sink. Here we investigate the drivers of FCO₂ at the seasonal scale with the aim of examining the mechanisms behind the observed biases in the Sub-Antarctic and Antarctic zone ... [123]

1177 [In this study we expand on the framework proposed by Mongwe et al. \(2016\), which examined the](#)
1178 [competing roles of temperature and DIC as drivers of pCO₂ variability and the seasonal cycle of pCO₂ in the](#)
1179 [Southern Ocean, to explain the mechanistic basis for seasonal biases of pCO₂ and FCO₂ between](#)
1180 [observational products and CMIP5 models. This analysis of 10 CMIP5 models and one observational](#)
1181 [product \(Landschutzer et al., 2014\) highlighted that although the models showed different seasonal modes](#)
1182 [\(Fig. 2\), they could be grouped into two categories \(SST- and DIC-driven\) according to their mean seasonal](#)
1183 [bias of temperature or DIC control \(Fig. 3 & 6\).](#)

V2 Changes 2018/3/6 6:53 PM
Formatted: normal, Right, Tabs: 7,62 cm, Centered + 15,24 cm, Right, Position:Horizontal: Left, Relative to: Column, Vertical: In line, Relative to: Margin, Wrap Around

1184 [A few general insights emerge from this analysis. Firstly, despite significant differences in the spatial](#)
1185 [characteristics of the mean annual fluxes \(Fig. 1\), models show unexpectedly greater inter-basin coherence](#)

V2 Changes 2018/3/6 6:53 PM
Formatted: Default Paragraph Font

1216 [in the phasing seasonal cycle of FCO₂ and SST-DIC control than observational products \(Fig. 3 & 6\). Clear](#)
1217 [inter-basin differences have been highlighted in studies on the climatology and interannual variability that](#)
1218 [examined pCO₂ and CO₂ fluxes based on data products \(Landschutzer et al., 2015; Gregor et al., 2017\) as](#)
1219 [well as phytoplankton chlorophyll based on remote sensing \(Thomalla et al., 2011; Carranza et al., 2016\).](#)
1220 [Briefly, the Atlantic Ocean shows the highest mean primary production in contrast to the Pacific Ocean,](#)
1221 [which has the lowest \(Thomalla et al., 2011\). Similarly, strong inter-basin differences for pCO₂ and FCO₂](#)
1222 [have been highlighted and ascribed to SST control \(Landschützer et al., 2016\) and wind stress - mixed layer](#)
1223 [depth \(Gregor et al., 2017\). The combined effect of these regional differences in forcing of pCO₂ and FCO₂](#)
1224 [would be expected to be reflected in the CMIP5 models as well. A quantitative analysis of the correlation](#)
1225 [of the phasing of the seasonal cycle of FCO₂ between basins for different models shows that all the models](#)
1226 [except 3 \(CMCC-CESM, GFDL-ESM2M CESM1-CESM\) are characterized by strong inter-basin correlation in](#)
1227 [both the SAZ and the AZ \(Fig. 4\). This suggests that the carbon cycle in these CMIP5 models is not sensitive](#)
1228 [to inter-basin differences in the drivers as is the case for observations.](#)

1230 [Secondly, an important part of this analysis is based on the assumption that the observational products](#)
1231 [that are used to constrain the spatial and temporal variability of pCO₂ and FCO₂ reflect the correct seasonal](#)
1232 [modes of the Southern Ocean. This assumption requires significant caution not only due to the limitations](#)
1233 [in the sparseness of the *in situ* observations but also due to limitations of the empirical techniques in](#)
1234 [overcoming these data gaps \(Landschutzer et al., 2014; Rödenbeck et al., 2015; Gregor et al., 2017a,b;](#)
1235 [Ritter et al., 2018\). The uncertainty analysis from these studies suggests that, while the seasonal bias in](#)
1236 [observations may be less in the SAZ and PFZ, it is the highest in the AZ where access is limited mostly to](#)
1237 [summer, and winter ice cover result in uncertainties that may limit the significance of the data - model](#)
1238 [comparisons. It is important to note that though the observation product we use here \(Landschützer et al.,](#)
1239 [2014\) is based on more surface measurement \(10 millions, SOCAT v3\) compared to previous datasets \(e.g.](#)
1240 [Takahashi et al., 2009, 3 millions\), the data are still sparse in time and space in the Southern Ocean. Thus](#)
1241 [using this data product as our main observational estimates for this analysis we are mindful of the](#)
1242 [limitations in its discussion below.](#)

1244 [Thirdly, the seasonal cycle of ΔpCO₂ is the dominant mode of variability in FCO₂ \(Mongwe et al., 2016;](#)
1245 [Wanninkhof et al., 2009\). Though winds provide the kinematic forcing for air-sea fluxes of CO₂ and](#)
1246 [indirectly affect FCO₂ through mixed layer dynamics and associated biogeochemical responses \(Mahadevan](#)
1247 [et al., 2012; du Plessis et al., 2017\), ΔpCO₂ sets the direction of the flux. Surface pCO₂ changes are mainly](#)
1248 [driven by DIC and SST \(Hauck et al., 2015; Takahashi et al., 1993\). Subsequently the sensitivity of CMIP5](#)
1249 [models to how changes in DIC and SST regulates seasonal cycle of FCO₂ is fundamental to the model's](#)

V2 Changes 2018/3/6 6:53 PM

Formatted: normal, Right, Tabs: 7,62 cm, Centered + 15,24 cm, Right, Position:Horizontal: Left, Relative to: Column, Vertical: In line, Relative to: Margin, Wrap Around

V2 Changes 2018/3/6 6:53 PM

Formatted: Default Paragraph Font

1250 ability to resolve observed FCO_2 seasonal cycle. Thus here we examined the influence of DIC and SST on
1251 FCO_2 at seasonal scale for 10 CMIP5 models with respect to observed estimates. But because temperature
1252 does not directly affects DIC changes, we first scaled up the impact of SST changes on pCO_2 through surface
1253 CO_2 solubility to equivalent DIC units using the Revelle factor (section 2.3). In this way we can distinguish
1254 the influence of surface solubility and DIC changes (i.e. biological and physical) on pCO_2 and hence then
1255 FCO_2 .

1256
1257 Fourthly, using this analysis framework (sec 2.3, summarized in Fig. 6) we found that CMIP5 models FCO_2
1258 biases cluster in two groups, namely group-DIC ($M_{\text{T-DIC}} < 0$) and group-SST ($M_{\text{T-DIC}} > 0$). Group-DIC models are
1259 characterized by an overestimation of the influence of DIC on pCO_2 with respect to observations estimates,
1260 which instead indicate that physical and biogeochemical changes in the DIC concentration mostly regulate
1261 the seasonal cycle of FCO_2 (in short, DIC control). Group-SST models show an excessive temperature
1262 influence on pCO_2 ; here surface CO_2 solubility biases are mainly responsible for the departure of modeled
1263 FCO_2 from the observational products. While CMIP5 models mostly show a singular dominant influence of
1264 these extremes, observations show a modest influence of both, with a dominance of DIC changes as the
1265 main driver of seasonal FCO_2 variability. Below we discuss the seasonal cycle characteristics and possible
1266 mechanisms for these two groups of CMIP5 models in the Sub-Antarctic and Antarctic Zones of the
1267 Southern Ocean.

1268 **4.1 Sub-Antarctic Zone (SAZ)**

1270
1271 Our diagnostic analysis indicates that the seasonal cycle of pCO_2 in the observational product (Landschützer
1272 et al., 2014) is mostly DIC controlled across all three basins of the SAZ ($M_{\text{T-DIC}} < 0$ in Fig. 6). The Atlantic
1273 Ocean shows a stronger DIC control (Annual mean $M_{\text{T-DIC}} \geq 2$) compared to the Pacific and Indian Ocean
1274 (Annual mean $M_{\text{T-DIC}} \approx 1$). This stronger influence of DIC on pCO_2 in the Atlantic Ocean is consistent with
1275 higher primary production in this basin (Graham et al., 2015; Thomalla et al., 2011), here shown by the
1276 larger mean seasonal chlorophyll from remote sensing in the Atlantic basin with respect to the Pacific and
1277 Indian basin (Fig. 8). This significant basin difference is most likely linked to a number of factors: the
1278 Atlantic basin has longer periods of shallow MLD compared to the Pacific and Indian basins (Fig. 7a-c, Nov –
1279 Mar & Nov - Feb respectively) and has been shown to have higher supplies of continental shelves and land
1280 based iron (Boyd and Ellwood, 2010; Tagliabue et al., 2012; 2014). These conditions are more likely to
1281 enhance primary production that translates into a higher rate of change of surface DIC (Fig. 8), which
1282 becomes the major driver of FCO_2 variability. In contrast, shorter periods of shallow MLD and lower iron
1283 inputs in the Pacific Ocean (Tagliabue et al., 2012), likely account for lower chlorophyll biomass and hence

V2 Changes 2018/3/6 6:53 PM

Formatted: normal, Right, Tabs: 7,62 cm, Centered + 15,24 cm, Right, Position: Horizontal: Left, Relative to: Column, Vertical: In line, Relative to: Margin, Wrap Around

V2 Changes 2018/3/6 6:53 PM

Formatted: Default Paragraph Font

1284 [the weaker DIC control evidenced in our analysis \(\$M_{T-DIC} \approx 0\$ in Fig. 6\). In the Indian Ocean, the winter mixed](#)
1285 [layer is deeper than in the Atlantic and deepens earlier in the season \(Fig. 7c\). These conditions limit](#)
1286 [chlorophyll concentration \(Fig. 8\) and possibly contribute to the lower rates of surface temperature change](#)
1287 [because of the enhanced mixing \(cf Fig. 5a-c\). As a consequence the resulting net driver in the Indian and](#)
1288 [Pacific basins is a weaker DIC control, because both biological DIC and solubility changes are relatively](#)
1289 [weaker and they oppose each other. Because of this, when the magnitudes of the rate of change of SST are](#)
1290 [larger during cooling and warming seasonal peaks \(autumn and spring respectively\), DIC control is weaker](#)
1291 [\(\$M_{T-DIC} \approx 0\$ \) during these seasons.](#)

1292
1293 [CMIP5 models do not capture these basin-specific features as demonstrated with the correlation analysis in](#)
1294 [Fig. 4, with the exception of three group-SST models \(i.e. CESM1-BGC, GFDL-ESM2M and CMCC-CESM\).](#)
1295 [These, in contrast, mostly show comparable \$FCO_2\$ phasing in the three basins. This spatial uniformity of](#)
1296 [CMIP5 models is both zonal and meridional for most models in the Southern Ocean \(Fig. 3, 4\), which is in](#)
1297 [contrast to observation products \(Fig. 3\). This suggests that CMIP5 models show equal sensitivity to basin](#)
1298 [scale \$FCO_2\$ drivers, suggesting that \$pCO_2\$ and \$FCO_2\$ driving mechanisms are less local than for observations.](#)

1299
1300 [The major feature of group-SST models in the SAZ is the outgassing during summer and ingassing in winter](#)
1301 [\(Fig. 3a-c, Dec-Feb\), which our diagnostics in Fig. 6 attribute to temperature \(solubility\) control. The](#)
1302 [summer period coincides with the highest warming rates \(\$dSST/dt\$, Fig 5a-c\), and associated reduction in](#)
1303 [solubility of \$CO_2\$. Similarly, exaggerated cooling rates at the onset of autumn \(Fig. 5a-c\) enhance \$CO_2\$](#)
1304 [solubility causing a change in the direction of \$FCO_2\$ into strengthening \$CO_2\$ ingassing \(Fig 3a-c\). Thus, while](#)
1305 [group-SST models have seasonal amplitude of \$FCO_2\$ comparable to observations, they are out of phase \(Fig.](#)
1306 [3\) as was the case in a previous analysis of a forced ocean model \(Mongwe et al., 2016\).](#)

1307
1308 [In addition to increasing \$CO_2\$ solubility, the rapid cooling at the onset of autumn also deepens the MLD](#)
1309 [\(March-June, Fig. 7\), which induces entrainment of DIC, increasing surface \$CO_2\$ concentration and](#)
1310 [weakening the ocean-atmosphere gradient and, in some instances, reversing the air-sea flux to outgassing](#)
1311 [\(Lenton et al., 2013a; Mahadevan et al., 2011; Metzl et al., 2006\). While these processes \(cooling and DIC](#)
1312 [entrainment\) are likely to co-occur in the Southern Ocean, in CMIP5 models they are characterized by their](#)
1313 [extremes: temperature impact of solubility exceeds the rate of entrainment \(Fig. 6 & 10\). Because of the](#)
1314 [dominance of the solubility effect in group-SST models, the impact of DIC entrainment on surface \$pCO_2\$](#)
1315 [changes, the weakening of \$CO_2\$ ingassing / outgassing only happens in mid-late winter \(June-July -August\)](#)
1316 [when entrainment fluxes peak \(Fig. 10\) and the SST rate approaches zero \(Fig. 5\).](#)

1317

V2 Changes 2018/3/6 6:53 PM

Formatted: normal, Right, Tabs: 7,62 cm, Centered + 15,24 cm, Right, Position:Horizontal: Left, Relative to: Column, Vertical: In line, Relative to: Margin, Wrap Around

V2 Changes 2018/3/6 6:53 PM

Formatted: Default Paragraph Font

1318
1319 [In the spring-summer transition, primary production is anticipated to enhance the net CO₂ uptake](#)
1320 [\(Thomalla et al., 2011; Le Quéré and Saltzman, 2013\). However, the elevated surface warming rates during](#)
1321 [spring reduces CO₂ solubility in group-SST models and overwhelms the role of primary production in the](#)
1322 [seasonal cycle of pCO₂ and fCO₂ \(atmospheric CO₂ uptake\). As a consequence, these group-SST models](#)
1323 [mostly show a constant or weakening net CO₂ uptake flux during spring in the Pacific and Atlantic Ocean](#)
1324 [even though primary production is occurring and is relatively elevated \(Fig. 3 & 8\). Though some models](#)
1325 [show chlorophyll concentrations comparable to observations \(e.g. GFDL-ESM2M, CNRM-CM5, CanESM2\),](#)
1326 [and sometimes greater \(e.g. MRI-ESM\), the impact of temperature driven solubility dominates due the](#)
1327 [phasing of the rates of the two drivers \(Fig. 2a-c\). The Indian Ocean however shows the only exception to](#)
1328 [this phenomenon. Here, the amplitude of the seasonal surface warming is relatively smaller \(~ 0.5 °C⁻¹](#)
1329 [month⁻¹ lower than the Pacific and Atlantic basins\), and the biologically driven CO₂ uptake becomes notable](#)
1330 [and show a net strengthening of the sink of CO₂ during spring \(Fig. 3c\).](#)

1331
1332 [Though almost all analysed CMIP5 models \(with the exception of NorESM1-ME\) exaggerate the warming](#)
1333 [and cooling rates in autumn and spring, group-DIC models do not manifest the expected temperature-](#)
1334 [driven solubility impact on pCO₂ and fCO₂ \(Fig. 2\) Instead, the seasonal cycle of pCO₂ and fCO₂ are](#)
1335 [controlled by DIC changes. However, this is driven by an overestimated seasonal primary production and](#)
1336 [the associated carbon export fluxes \(Fig. 8\). It is striking how in these models the seasonal cycle of](#)
1337 [chlorophyll and fCO₂ are in phase \(Fig 3a-c, 8a-c, with linear correlation coefficients always larger than 0.9,](#)
1338 [not shown\) but, as we discuss below, this is not because the temperature rates of change are correctly](#)
1339 [scaled but because the biogeochemical process rates are exaggerated \(Fig. 8\).](#)

1340
1341 [Because of the particularly enhanced production in group-DIC models, the CO₂ sink is stronger \(Fig. 8\) with](#)
1342 [respect to observation estimates during spring. This is visible in the reduction of surface DIC \(negative](#)
1343 [dDIC/dt in Fig. 8a, g-i\), which can only be explained by drawdown due to the formation and export of](#)
1344 [organic matter \(Le Quéré and Saltzman, 2013\). However, note that in the same way, after the December](#)
1345 [production peak, both CMIP5 models and observations show an increase of surface DIC concentrations](#)
1346 [\(positive dDIC/dt\) until March \(Fig. 8, g-i\). These DIC growth rates are particularly enhanced in group-DIC](#)
1347 [models compared to some group-SST and observations \(Fig. S9\). The onset of these DIC increases also](#)
1348 [coincides with the depletion of surface oxygen \(Fig. S9\), which we makes us speculate that this is due to the](#)
1349 [remineralisation of organic matter to DIC through respiration. Unfortunately, only a few models have](#)
1350 [stored the respiration rates, therefore the ultimate reason for this DIC rebound remains to be examined at](#)
1351 [a later stage. We would however tend to exclude other processes, because the onset of CO₂ outgassing](#)

V2 Changes 2018/3/6 6:53 PM

Formatted: normal, Right, Tabs: 7,62 cm, Centered + 15,24 cm, Right, Position:Horizontal: Left, Relative to: Column, Vertical: In line, Relative to: Margin, Wrap Around

V2 Changes 2018/3/6 6:53 PM

Formatted: Default Paragraph Font

1352 [seen in March in group-DIC models occurs prior to significant MLD deepening \(Fig. 7\) and entrainment](#)
1353 [fluxes, therefore remineralization is likely be a key process here \(Fig. 8\).](#)

1354

1355 [4.2 Antarctic Zone \(AZ\)](#)

1356

1357 [The seasonal cycle framework summarized in Fig. 6 shows that the variability of \$FCO_2\$ and \$pCO_2\$ in the](#)
1358 [Landschützer et al. \(2014\) product is characterized by a stronger DIC control \(annual mean \$M_{T-DIC} < -2\$ \)](#)
1359 [relative to the Sub-Antarctic \(\$M_{T-DIC} \approx -1\$ \), except in the spring season \(\$M_{T-DIC} > -1\$ \). This DIC control is](#)
1360 [spatially uniform in the Antarctic zone across all three basins \(Fig. 4\). The available datasets indicate that](#)
1361 [the combination of weaker SST rates due to lower solar heating fluxes \(Fig. 5\), and stronger shallower](#)
1362 [vertical DIC maxima \(Fig. 10\) favour a stronger DIC control through larger surface DIC rates. The spatial](#)
1363 [uniformity in the seasonality of \$FCO_2\$ is also evident in the satellite chlorophyll and calculated \$dDIC/dt\$ from](#)
1364 [GLODAP2 in Fig. 9. Contrary to the Sub-Antarctic this might be suggesting that \$FCO_2\$ mechanisms are here](#)
1365 [less local. It could be hypothesized that the seasonal extent of sea-ice, deeper mixing and heat balance](#)
1366 [differences affect this region more uniformly compared to the Sub-Antarctic zone, and hence the](#)
1367 [mechanisms of \$FCO_2\$ are spatially homogeneous. However, we cannot forget that sparseness of](#)
1368 [observations in this region is a known key limitation to data products \(Bakker et al., 2014; Gregor et al.,](#)
1369 [2017; Monteiro et al., 2010; Rödenbeck et al., 2013\) that might hamper the emergence of basin specific](#)
1370 [features. Consequently, this highlights the importance and need to prioritize independent observations in](#)
1371 [the Southern Ocean south of the polar front and in the Marginal Ice Zone. Increased observational efforts](#)
1372 [should also include a variety of platforms such as autonomous vehicles like gliders \(Monteiro et al., 2015\)](#)
1373 [and biogeochemical floats \(Johnson et al., 2017\) in addition to ongoing ship-based measurements.](#)

1374

1375 [In general terms, CMIP5 models are mostly in agreement \(with an exception of MRI-ESM\) with the](#)
1376 [observational product on the dominant role of DIC to regulating the seasonal cycle of \$FCO_2\$ \(Fig. 6d-f\),](#)
1377 [though not all models agree in the phase of the seasonal cycle of \$FCO_2\$ \(e.g. CanESM2, Fig. 2\). Though](#)
1378 [CMIP5 models still mostly show the SST rates biases in autumn and spring with respect to observed](#)
1379 [estimates, the stronger and near surface vertical DIC maxima \(Fig. 10\), likely favor DIC as a dominant driver](#)
1380 [of \$FCO_2\$ changes. , Differences between group-SST and group-DIC models are only evident in mid-summer](#)
1381 [when SST rates heighten and primary production peaks \(Fig. 3 & 9\). Probably because of sea ice presence,](#)
1382 [the onset of SST warming is a month later \(November\) here in comparison to the Sub-Antarctic \(October\).](#)
1383 [This subsequently allows the onset of primary production before the surface warming, which then permits](#)
1384 [the biological \$CO_2\$ uptake to be notable in group-SST models. We notice here that the reason why CMIP5](#)
1385 [models develop a winter bloom in the AZ requires further investigation \(Hague and Vichi, submitted\). Thus](#)

V2 Changes 2018/3/6 6:53 PM

Formatted: normal, Right, Tabs: 7,62 cm, Centered + 15,24 cm, Right, Position:Horizontal: Left, Relative to: Column, Vertical: In line, Relative to: Margin, Wrap Around

V2 Changes 2018/3/6 6:53 PM

Formatted: Default Paragraph Font

1386 [the two model groups here agree in the FCO₂ ingassing during spring with group-SST models being the](#)
1387 [closest to the observational product. The MRI-ESM is the only model showing anomalous solubility](#)
1388 [dominance during autumn and spring as in the Sub-Antarctic zone.](#)

1389 [This coherence of CMIP5 models and observations in the Antarctic zone, may suggest that CMIP5 models](#)
1390 [compare better to observations in this region \(Fig. 4\). However, because CMIP5 models also show this](#)
1391 [spatial homogeneity in the Sub-Antarctic Zone \(contrary to observational estimates\), it not clear whether](#)
1392 [this indicates an improved skill in CMIP5 model to the mechanisms of FCO₂ in this region, or both CMIP5](#)
1393 [models and observational product lacks spatial sensitivity to the drivers of FCO₂. The sparseness of](#)
1394 [observations in the AZ points to the latter.](#)

1397 [5. Synthesis](#)

1398
1399 [We used a seasonal cycle framework to highlight and examine two major biases in respect of pCO₂ and](#)
1400 [FCO₂ in 10 CMIP5 models in the Southern Ocean.](#)

1401
1402 [Firstly, the general exaggeration of the seasonal rates of change of SST in autumn and spring seasons during](#)
1403 [peak cooling and warming respectively with respect to available observations. These elevated rates of SST](#)
1404 [change tip the control of the seasonal cycle of pCO₂ and FCO₂ towards SST from DIC and result in a](#)
1405 [divergence between the observed and modelled seasonal cycles, particularly in the Sub-Antarctic Zone.](#)

1406 [While almost all analysed models \(9 of 10\) show these SST-driven biases, 3 of the 10 \(namely NorESM1-ME,](#)
1407 [HadGEM-ES and MPI-ESM\) don't show these solubility biases because of their overly exaggerated primary](#)
1408 [production \(and remineralization\) rates such that biologically driven DIC changes mainly regulate the](#)
1409 [seasonal cycle of FCO₂. These models reproduce the observed phasing of FCO₂ as a result of an incorrect](#)
1410 [scaling of the biogeochemical fluxes. In the Antarctic zone, CMIP5 models compare better with](#)
1411 [observations relative to the Sub-Antarctic Zone. This is mostly because both CMIP5 models and](#)
1412 [observational product estimates show a spatial and temporal uniformity in the characteristics of FCO₂ in](#)
1413 [the Antarctic zone. However, it is not certain if this is because model process dynamics perform better in](#)
1414 [this high latitude zone or that the observational products variability is itself limited by the lack of *in situ*](#)
1415 [data. This remains an open question that needs to be explored further and highlights the need for](#)
1416 [increased scale sensitive and independent observations south of the Polar Front and into the sea ice zone.](#)

1417
1418 [The second major bias is that contrary to observational products estimates, CMIP5 models generally show](#)
1419 [an equal sensitivity to basin scale FCO₂ drivers \(except for CMCC-ESM, GFDL-ESM2M and CESM1-BGC\) and](#)

V2 Changes 2018/3/6 6:53 PM

Formatted: normal, Right, Tabs: 7,62 cm, Centered + 15,24 cm, Right, Position:Horizontal: Left, Relative to: Column, Vertical: In line, Relative to: Margin, Wrap Around

V2 Changes 2018/3/6 6:53 PM

Formatted: Default Paragraph Font

1420 [hence the seasonal cycle of FCO₂ has similar phasing in all three basins of the Sub-Antarctic zone. This is in](#)
1421 [contrast to observational and remote sensing products that highlight strong seasonal and interannually](#)
1422 [varying basin contrasts in both pCO₂ and phytoplankton biomass. It is not clear if this is due to inadequate](#)
1423 [carbon process parameterization or gaps in the dynamics of the physics. This should be investigated](#)
1424 [further with CMIP6 models and our analysis framework is proposed as a useful tool to diagnose the](#)
1425 [dominant drivers. Contrary to observed estimates, CMIP5 models simulate FCO₂ seasonal dynamics that](#)
1426 [are zonally homogeneous and for this reason it is suggested that any investigation of local \(basin scale\)](#)
1427 [mechanisms, dynamics and long term trends of FCO₂ using CMIP5 models should be cautious. This](#)
1428 [highlights a key area of development for CMIP6.](#)

1430 [Acknowledgements](#)

1431
1432 [This work was undertaken with financial support from the following South African institutions: CSIR](#)
1433 [Parliamentary Grant, National Research Foundation \(NRF SANAP programme\), Department of Science and](#)
1434 [Technology South Africa \(DST\), and the Applied Centre for Climate and Earth Systems Science \(ACCESS\). We](#)
1435 [thank the CSIR Centre for High Performance Computing \(CHPC\) for providing the resources for doing this](#)
1436 [analysis. We also want to thank Peter Landschützer, Taro Takahashi and Luke Gregor for making their data](#)
1437 [products available as well as the three reviewers for their productive comments that we think have](#)
1438 [strengthened the paper](#)

1445 [References](#)

1446 [Anav, A., Friedlingstein, P., Kidston, M., Bopp, L., Ciais, P., Cox, P., Jones, C., Jung, M., Myneni, R. and Zhu,](#)
1447 [Z.: Evaluating the land and ocean components of the global carbon cycle in the CMIP5 earth system models,](#)
1448 [J. Clim., 26\(18\), 6801–6843, doi:10.1175/JCLI-D-12-00417.1, 2013.](#)

V2 Changes 2018/3/6 6:53 PM

Formatted: normal, Right, Tabs: 7,62 cm, Centered + 15,24 cm, Right, Position:Horizontal: Left, Relative to: Column, Vertical: In line, Relative to: Margin, Wrap Around

V2 Changes 2018/3/6 6:53 PM

Formatted: Default Paragraph Font

1451 [Bakker, D. C. E., Pfeil, B., Smith, K., Hankin, S., Olsen, A., Alin, S. R., Cosca, C., Harasawa, S., Kozyr, A., Nojiri,](#)
1452 [Y., O'Brien, K. M., Schuster, U., Telszewski, M., Tilbrook, B., Wada, C., Akl, J., Barbero, L., Bates, N. R.,](#)
1453 [Boutin, J., Bozec, Y., Cai, W.-J., Castle, R. D., Chavez, F. P., Chen, L., Chierici, M., Currie, K., De Baar, H. J. W.,](#)
1454 [Evans, W., Feely, R. A., Fransson, A., Gao, Z., Hales, B., Hardman-Mountford, N. J., Hoppema, M., Huang,](#)
1455 [W.-J., Hunt, C. W., Huss, B., Ichikawa, T., Johannessen, T., Jones, E. M., Jones, S. D., Jutterström, S., Kitidis,](#)
1456 [V., Körtzinger, A., Landschützer, P., Lauvset, S. K., Lefèvre, N., Manke, A. B., Mathis, J. T., Merlivat, L., Metzl,](#)
1457 [N., Murata, A., Newberger, T., Omar, A. M., Ono, T., Park, G.-H., Paterson, K., Pierrot, D., Ríos, A. F., Sabine,](#)
1458 [C. L., Saito, S., Salisbury, J., Sarma, V. V. S. S., Schlitzer, R., Sieger, R., Skjelvan, I., Steinhoff, T., Sullivan, K. F.,](#)
1459 [Sun, H., Sutton, A. J., Suzuki, T., Sweeney, C., Takahashi, T., Tjiputra, J. F., Tsurushima, N., Van Heuven, S. M.](#)
1460 [A. C., Vandemark, D., Vlahos, P., Wallace, D. W. R., Wanninkhof, R. H. and Watson, A. J.: An update to the](#)
1461 [surface ocean CO₂ 2 \$\delta\$ atlas \(SOCAT version 2\), Earth Syst. Sci. Data, 6\(1\), 69–90, doi:10.5194/essd-6-69-](#)
1462 [2014, 2014.](#)

1463

1464 [Barbero, L., Boutin, J., Merlivat, L., Martin, N., Takahashi, T., Sutherland, S. C. and Wanninkhof, R.:](#)
1465 [Importance of water mass formation regions for the air-sea CO₂ flux estimate in the southern ocean, Global](#)
1466 [Biogeochem. Cycles, 25\(1\), 1–16, doi:10.1029/2010GB003818, 2011.](#)

1467

1468 [Boyd, P. W. and Ellwood, M. J.: The biogeochemical cycle of iron in the ocean, Nat. Geosci., 3\(10\), 675–682,](#)
1469 [doi:10.1038/ngeo964, 2010.](#)

1470

1471 [de Boyer Montégut, C., Madec, G., Fischer, A. S., Lazar, A. and Iudicone, D.: Mixed layer depth over the](#)
1472 [global ocean: An examination of profile data and a profile-based climatology, J. Geophys. Res. C Ocean.,](#)
1473 [109\(12\), 1–20, doi:10.1029/2004JC002378, 2004.](#)

1474

1475 [Dickson, A. G. and Millero, F. J.: A comparison of the equilibrium constants for the dissociation of carbonic](#)
1476 [acid in seawater media, Deep Sea Res. Part A, Oceanogr. Res. Pap., 34\(10\), 1733–1743, doi:10.1016/0198-](#)
1477 [0149\(87\)90021-5, 1987.](#)

1478

1479 [Dufour, C. O., Sommer, J. Le, Gehlen, M., Orr, J. C., Molines, J. M., Simeon, J. and Barnier, B.: Eddy](#)
1480 [compensation and controls of the enhanced sea-to-air CO₂ flux during positive phases of the Southern](#)
1481 [Annular Mode, Global Biogeochem. Cycles, 27\(3\), 950–961, doi:10.1002/gbc.20090, 2013.](#)

1482

1483 [Feely, R. A., Wanninkhof, R., McGillis, W., Carr M. E and Cosca, C.: Effects of wind speed and gas exchange](#)
1484 [parameterizations on the air-sea CO₂ fluxes in the equatorial Pacific Ocean, J. Geophys. Res., 109\(C8\),](#)

V2 Changes 2018/3/6 6:53 PM

Formatted: normal, Right, Tabs: 7,62 cm, Centered + 15,24 cm, Right, Position:Horizontal: Left, Relative to: Column, Vertical: In line, Relative to: Margin, Wrap Around

V2 Changes 2018/3/6 6:53 PM

Formatted: Default Paragraph Font

1485 [C08S03, doi:10.1029/2003JC001896, 2004.](#)

1486

1487 [Frölicher, T. L., Sarmiento, J. L., Paynter, D. J., Dunne, J. P., Krasting, J. P. and Winton, M.: Dominance of the](#)

1488 [Southern Ocean in anthropogenic carbon and heat uptake in CMIP5 models, J. Clim., 28\(2\), 862–886,](#)

1489 [doi:10.1175/JCLI-D-14-00117.1, 2015.](#)

1490

1491 [Fung, I. Y., Doney, S. C., Lindsay, K. and John, J.: Evolution of carbon sinks in a changing climate, Proc. Natl.](#)

1492 [Acad. Sci., 102\(32\), 11201–11206, doi:10.1073/pnas.0504949102, 2005.](#)

1493

1494 [Graham, R. M., De Boer, A. M., van Sebille, E., Kohfeld, K. E. and Schlosser, C.: Inferring source regions and](#)

1495 [supply mechanisms of iron in the Southern Ocean from satellite chlorophyll data, Deep. Res. Part I](#)

1496 [Oceanogr. Res. Pap., 104, 9–25, doi:10.1016/j.dsr.2015.05.007, 2015.](#)

1497

1498 [Gregor, L., Kok, S. and Monteiro, P. M. S.: Empirical methods for the estimation of Southern Ocean CO₂:](#)

1499 [support vector and random forest regression, Biogeosciences, 14\(23\), 5551–5569, doi:10.5194/bg-14-5551-](#)

1500 [2017, 2017a.](#)

1501

1502 [Gregor, L., Kok, S. and Monteiro, P. M. S.: Interannual drivers of the seasonal cycle of CO₂ fluxes in the](#)

1503 [Southern Ocean, Biogeosciences Discuss., \(September\), 1–28, doi:10.5194/bg-2017-363, 2017b.](#)

1504

1505 [Gruber, N., Gloor, M., Mikaloff Fletcher, S. E., Doney, S. C., Dutkiewicz, S., Follows, M. J., Gerber, M.,](#)

1506 [Jacobson, A. R., Joos, F., Lindsay, K., Menemenlis, D., Mouchet, A., Müller, S. A., Sarmiento, J. L. and](#)

1507 [Takahashi, T.: Oceanic sources, sinks, and transport of atmospheric CO₂, Global Biogeochem. Cycles, 23\(1\),](#)

1508 [1–21, doi:10.1029/2008GB003349, 2009.](#)

1509

1510 [Hauck, J. and Völker, C.: A multi-model study on the Southern Ocean CO₂ uptake and the role of the](#)

1511 [biological carbon pump in the 21st century, EGU Gen. Assem., 17, 12225,](#)

1512 [doi:10.1002/2015GB005140.Received, 2015.](#)

1513 [Hauck, J., Völker, C., Wolf-Gladrow, D. a., Laufkötter, C., Vogt, M., Aumont, O., Bopp, L., Buitenhuis, E. T.,](#)

1514 [Doney, S. C., Dunne, J., Gruber, N., John, J., Le Quééré, C., Lima, I. D., Nakano, H. and Totterdell, I.: On the](#)

1515 [Southern Ocean CO₂ uptake and the role of the biological carbon pump in the 21st century, Global](#)

1516 [Biogeochem. Cycles, 29, 1451–1470, doi:doi:10.1002/2015GB005140, 2015.](#)

1517

1518 [Ilyina, T., Six, K. D., Segschneider, J., Maier-Reimer, E., Li, H. and Núñez-Riboni, I.: Global ocean](#)

V2 Changes 2018/3/6 6:53 PM

Formatted: normal, Right, Tabs: 7,62 cm, Centered + 15,24 cm, Right, Position:Horizontal: Left, Relative to: Column, Vertical: In line, Relative to: Margin, Wrap Around

V2 Changes 2018/3/6 6:53 PM

Formatted: Default Paragraph Font

1519 [biogeochemistry model HAMOCC: Model architecture and performance as component of the MPI-Earth](#)
1520 [system model in different CMIP5 experimental realizations, J. Adv. Model. Earth Syst., 5\(2\), 287–315,](#)
1521 [doi:10.1029/2012MS000178, 2013.](#)

1522
1523 [Johnson, K. S., Plant, J. N., Coletti, L. J., Jannasch, H. W., Sakamoto, C. M., Riser, S. C., Swift, D. D., Williams,](#)
1524 [N. L., Boss, E., Haëntjens, N., Talley, L. D. and Sarmiento, J. L.: Biogeochemical sensor performance in the](#)
1525 [SOCCOM profiling float array, J. Geophys. Res. Ocean., \(September\), doi:10.1002/2017JC012838, 2017.](#)

1526
1527 [Johnson, R., Strutton, P. G., Wright, S. W., McMinn, A. and Meiners, K. M.: Three improved satellite](#)
1528 [chlorophyll algorithms for the Southern Ocean, J. Geophys. Res. Ocean., 118\(7\), 3694–3703,](#)
1529 [doi:10.1002/jgrc.20270, 2013.](#)

1530
1531 [Kessler, A. and Tjiputra, J.: The Southern Ocean as a constraint to reduce uncertainty in future ocean](#)
1532 [carbon sinks, Earth Syst. Dyn., 7\(2\), 295–312, doi:10.5194/esd-7-295-2016, 2016.](#)

1533
1534 [Landschützer, P., Gruber, N. and Bakker, D. C. E. Stemmler, I. and Six, K. D.: Strengthening seasonal marine](#)
1535 [CO2 variations due to increasing atmospheric CO2. Nature Climate Change, 8, 146-150, Doi:](#)
1536 [10.1038/s41558-017-0057-x, 2018.](#)

1537
1538 [Landschützer, P., Gruber, N. and Bakker, D. C. E.: Decadal variations and trends of the global ocean carbon](#)
1539 [sink, Global Biogeochem. Cycles, 30\(10\), 1396–1417, doi:10.1002/2015GB005359, 2016.](#)

1540
1541 [Landschützer, P., Gruber, N., Haumann, F. A., Rodenbeck, C., Bakker, D. C. E., van Heuven, S., Hoppema, M.,](#)
1542 [Metz, N., Sweeney, C., Takahashi, T., Tilbrook, B. and Wanninkhof, R.: The reinvigoration of the Southern](#)
1543 [Ocean carbon sink, Science \(80-. \), 349\(6253\), 1221–1224, doi:10.1126/science.aab2620, 2015.](#)

1544
1545 [Landschützer, P., Gruber, N., Bakker, D. C. E. and Schuster, U.: Recent variability of the global ocean carbon](#)
1546 [sink, Glob. Planet. Change, 927–949, doi:10.1002/2014GB004853.Received, 2014.](#)

1547
1548 [Lauvset, S. K., Key, R. M., Olsen, A., Van Heuven, S., Velo, A., Lin, X., Schirnick, C., Kozyr, A., Tanhua, T.,](#)
1549 [Hoppema, M., Jutterström, S., Steinfeldt, R., Jeansson, E., Ishii, M., Perez, F. F., Suzuki, T. and Watelet, S.: A](#)
1550 [new global interior ocean mapped climatology: The 1° × 1° GLODAP version 2, Earth Syst. Sci. Data, 8\(2\),](#)
1551 [325–340, doi:10.5194/essd-8-325-2016, 2016.](#)

1552

V2 Changes 2018/3/6 6:53 PM

Formatted: normal, Right, Tabs: 7,62 cm, Centered + 15,24 cm, Right, Position:Horizontal: Left, Relative to: Column, Vertical: In line, Relative to: Margin, Wrap Around

V2 Changes 2018/3/6 6:53 PM

Formatted: Default Paragraph Font

1553 [Lee, K., Tong, L. T., Millero, F. J., Sabine, C. L., Dickson, A. G., Goyet, C., Park, G. H., Wanninkhof, R., Feely, R.](#)
1554 [A. and Key, R. M.: Global relationships of total alkalinity with salinity and temperature in surface waters of](#)
1555 [the world's oceans, Geophys. Res. Lett., 33\(19\), 1–5, doi:10.1029/2006GL027207, 2006.](#)

1556

1557 [Lenton, A., Metzl, N., Takahashi, T., Kuchinke, M., Matear, R. J., Roy, T., Sutherland, S. C., Sweeney, C. and](#)
1558 [Tilbrook, B.: The observed evolution of oceanic pCO₂ and its drivers over the last two decades, Global](#)
1559 [Biogeochem. Cycles, 26\(2\), 1–14, doi:10.1029/2011GB004095, 2012.](#)

1560

1561 [Lenton, A., Tilbrook, B., Law, R., Bakker, D., Doney, S. C., Gruber, N., Hoppema, M., Ishii, M., Lovenduski, N.](#)
1562 [S., Matear, R. J., McNeil, B. I., Metzl, N., Mikaloff Fletcher, S. E., Monteiro, P., Rödenbeck, C., Sweeney, C.](#)
1563 [and Takahashi, T.: Sea-air CO₂ fluxes in the Southern Ocean for the period](#)
1564 [1990–2009, Biogeosciences Discuss., 10\(1\), 285–333, doi:10.5194/bgd-10-285-2013, 2013.](#)

1565

1566 [Leung, S., Cabre, A. and Marinov, I.: A latitudinally banded phytoplankton response to 21st century climate](#)
1567 [change in the Southern Ocean across the CMIP5 model suite, Biogeosciences, 12\(19\), 5715–5734,](#)
1568 [doi:10.5194/bg-12-5715-2015, 2015.](#)

1569

1570 [Locarnini, R. A., Mishonov, A. V., Antonov, J. I., Boyer, T. P., Garcia, H. E., Baranova, O. K., Zweng, M. M.,](#)
1571 [Paver, C. R., Reagan, J. R., Johnson, D. R., Hamilton, M. and Seidov, D.: World Ocean Atlas 2013. Vol. 1:](#)
1572 [Temperature., 2013.](#)

1573

1574 [Mahadevan, A., Tagliabue, A., Bopp, L., Lenton, A., Memery, L. and Levy, M.: Impact of episodic vertical](#)
1575 [fluxes on sea surface pCO₂, Philos. Trans. R. Soc. A Math. Phys. Eng. Sci., 369\(1943\), 2009–2025,](#)
1576 [doi:10.1098/rsta.2010.0340, 2011.](#)

1577

1578 [Mahadevan, A., D'Asaro, E., Lee, C. and Perry, M. J.: Eddy-driven stratification initiates North Atlantic spring](#)
1579 [phytoplankton blooms, Science \(80- \), 336\(6090\), 54–58, doi:10.1126/science.1218740, 2012.](#)

1580 [Marinov, I. and Gnanadesikan, A.: Changes in ocean circulation and carbon storage are decoupled from air-](#)
1581 [sea CO₂ fluxes, Biogeosciences, 8\(2\), 505–513, doi:10.5194/bg-8-505-2011, 2011.](#)

1582

1583 [Marinov, I., Gnanadesikan, A., Toggweiler, J. R. and Sarmiento, J. L.: The Southern Ocean biogeochemical](#)
1584 [divide, Nature, 441\(7096\), 964–967, doi:10.1038/nature04883, 2006.](#)

1585

1586 [Matear, R. J. and Lenton, A.: Impact of Historical Climate Change on the Southern Ocean Carbon Cycle, J.](#)

V2 Changes 2018/3/6 6:53 PM

Formatted: normal, Right, Tabs: 7,62 cm, Centered + 15,24 cm, Right, Position: Horizontal: Left, Relative to: Column, Vertical: In line, Relative to: Margin, Wrap Around

V2 Changes 2018/3/6 6:53 PM

Formatted: Default Paragraph Font

1587 [Clim., 21\(22\), 5820–5834, doi:10.1175/2008JCLI2194.1, 2008.](#)

1588

1589 [McNeil, B. I., Metzl, N., Key, R. M., Matear, R. J. and Corbiere, A.: An empirical estimate of the Southern](#)

1590 [Ocean air-sea CO2 flux, Global Biogeochem. Cycles, 21\(3\), 1–16, doi:10.1029/2007GB002991, 2007.](#)

1591

1592 [Mehrbach, C., Culberson, C. H., Hawley, J. E. and Pytkowicz, R. M.: Measurement of the Apparent](#)

1593 [Dissociation Constants of Carbonic Acid in Seawater At Atmospheric Pressure, Limnol. Oceanogr., 18\(6\),](#)

1594 [897–907, doi:10.4319/lo.1973.18.6.0897, 1973.](#)

1595

1596 [Metzl, N.: Decadal increase of oceanic carbon dioxide in Southern Indian Ocean surface waters \(1991-](#)

1597 [2007\), Deep. Res. Part II Top. Stud. Oceanogr., 56\(8–10\), 607–619, doi:10.1016/j.dsr2.2008.12.007, 2009.](#)

1598 [Metzl, N., Brunet, C., Jabaud-Jan, A., Poisson, A. and Schauer, B.: Summer and winter air-sea CO2 fluxes in](#)

1599 [the Southern Ocean, Deep. Res. Part I Oceanogr. Res. Pap., 53\(9\), 1548–1563,](#)

1600 [doi:10.1016/j.dsr.2006.07.006, 2006.](#)

1601

1602 [Mongwe, N. P., Chang, N. and Monteiro, P. M. S.: The seasonal cycle as a mode to diagnose biases in](#)

1603 [modelled CO2 fluxes in the Southern Ocean, Ocean Model., 106, 90–103,](#)

1604 [doi:10.1016/j.ocemod.2016.09.006, 2016.](#)

1605

1606 [Monteiro, P. M. S., Monteiro, P. M. S., Monteiro, P. M. S., Monteiro, P. M. S., Monteiro, P. M. S., Monteiro,](#)

1607 [P. M. S., Monteiro, P. M. S., Monteiro, P. M. S., Monteiro, P. M. S., Monteiro, P. M. S., Monteiro, P. M. S.,](#)

1608 [Monteiro, P. M. S. and Monteiro, P. M. S.: A Global Sea Surface Carbon Observing System: Assessment of](#)

1609 [Changing Sea Surface CO2 and Air-Sea CO2 Fluxes, Proc. Ocean. Sustain. Ocean Obs. Inf. Soc., \(1\), 702–714,](#)

1610 [doi:10.5270/OceanObs09.cwp.64, 2010.](#)

1611

1612 [Monteiro, P. M. S., Gregor, L., Lévy, M., Maenner, S., Sabine, C. L. and Swart, S.: Intra-seasonal variability](#)

1613 [linked to sampling alias in air – sea CO2 fluxes in the Southern Ocean, Geophys. Res. Lett., 1–8,](#)

1614 [doi:10.1002/2015GL066009, 2015.](#)

1615

1616 [Moore, J. K., Doney, S. C. and Lindsay, K.: Upper ocean ecosystem dynamics and iron cycling in a global](#)

1617 [three-dimensional model, Global Biogeochem. Cycles, 18\(4\), 1–21, doi:10.1029/2004GB002220, 2004.](#)

1618

1619 [Orsi, A. H., Whitworth, T. and Nowlin, W. D.: On the meridional extent and fronts of the Antarctic](#)

1620 [Circumpolar Current, Deep. Res. Part I, 42\(5\), 641–673, doi:10.1016/0967-0637\(95\)00021-W, 1995.](#)

V2 Changes 2018/3/6 6:53 PM

Formatted: normal, Right, Tabs: 7,62 cm, Centered + 15,24 cm, Right, Position: Horizontal: Left, Relative to: Column, Vertical: In line, Relative to: Margin, Wrap Around

V2 Changes 2018/3/6 6:53 PM

Formatted: Default Paragraph Font

1621
1622 [Pasquer, B., Metzl, N., Goosse, H. and Lancelot, C.: What drives the seasonality of air-sea CO₂ fluxes in the](#)
1623 [ice-free zone of the Southern Ocean: A 1D coupled physical-biogeochemical model approach, Mar. Chem.,](#)
1624 [177, 554–565, doi:10.1016/j.marchem.2015.08.008, 2015.](#)

1625
1626 [Pierrot, D. E. Lewis, and D. W. R. Wallace. 2006. MS Excel Program Developed for CO₂ System Calculations.](#)
1627 [ORNL/CDIAC-105a. Carbon Dioxide Information Analysis Center, Oak Ridge National Laboratory, U.S.](#)
1628 [Department of Energy, Oak Ridge, Tennessee. doi: 10.3334/CDIAC/otg.CO2SYS_XLS_CDIAC105a](#)

1629
1630 [du Plessis, M., Swart, S., Ansong, I. J. and Mahadevan, A.: Submesoscale processes promote seasonal](#)
1631 [restratification in the Subantarctic Ocean, J. Geophys. Res. Ocean., 122\(4\), 2960–2975,](#)
1632 [doi:10.1002/2016JC012494, 2017.](#)

1633
1634 [Le Quéré, C. and Saltzman, E. S.: Surface Ocean-Lower Atmosphere Processes., 2013.](#)

1635 [Le Quéré, C., Rödenbeck, C., Buitenhuis, E. T., Conway, T. J., Langenfelds, R., Gomez, A., Labuschagne, C.,](#)
1636 [Ramonet, M., Nakazawa, T., Metzl, N., Gillett, N. and Heimann, M.: Saturation of the southern ocean CO₂](#)
1637 [sink due to recent climate change, Science \(80-. \), 316\(5832\), 1735–1738, doi:10.1126/science.1136188,](#)
1638 [2007.](#)

1639
1640 [Le Quéré, C., Andrew, R. M., Canadell, J. G., Sitch, S., Ivar Korsbakken, J., Peters, G. P., Manning, A. C.,](#)
1641 [Boden, T. A., Tans, P. P., Houghton, R. A., Keeling, R. F., Alin, S., Andrews, O. D., Anthoni, P., Barbero, L.,](#)
1642 [Bopp, L., Chevallier, F., Chini, L. P., Ciais, P., Currie, K., Delire, C., Doney, S. C., Friedlingstein, P., Gkritzalis, T.,](#)
1643 [Harris, I., Hauck, J., Haverd, V., Hoppema, M., Klein Goldewijk, K., Jain, A. K., Kato, E., Körtzinger, A.,](#)
1644 [Landschützer, P., Lefèvre, N., Lenton, A., Lienert, S., Lombardozzi, D., Melton, J. R., Metzl, N., Millero, F.,](#)
1645 [Monteiro, P. M. S., Munro, D. R., Nabel, J. E. M. S., Nakaoka, S. I., O'Brien, K., Olsen, A., Omar, A. M., Ono,](#)
1646 [T., Pierrot, D., Poulter, B., Rödenbeck, C., Salisbury, J., Schuster, U., Schwinger, J., Séférian, R., Skjelvan, I.,](#)
1647 [Stocker, B. D., Sutton, A. J., Takahashi, T., Tian, H., Tilbrook, B., Van Der Laan-Luijkx, I. T., Van Der Werf, G.](#)
1648 [R., Viovy, N., Walker, A. P., Wiltshire, A. J. and Zaehle, S.: Global Carbon Budget 2016, Earth Syst. Sci. Data,](#)
1649 [8\(2\), 605–649, doi:10.5194/essd-8-605-2016, 2016.](#)

1650
1651 [Ritter, R., Landschützer, P., Gruber, N., Fay, A. R., Iida, Y., Jones, S., Nakaoka, S., Park, G. H., Peylin, P.,](#)
1652 [Rödenbeck, C., Rodgers, K. B., Shutler, J. D. and Zeng, J.: Observation-Based Trends of the Southern Ocean](#)
1653 [Carbon Sink, Geophys. Res. Lett., doi:10.1002/2017GL074837, 2017.](#)

1654

V2 Changes 2018/3/6 6:53 PM

Formatted: normal, Right, Tabs: 7,62 cm, Centered + 15,24 cm, Right, Position: Horizontal: Left, Relative to: Column, Vertical: In line, Relative to: Margin, Wrap Around

V2 Changes 2018/3/6 6:53 PM

Formatted: Default Paragraph Font

1655 [Rödenbeck, C., Keeling, R. F., Bakker, D. C. E., Metzl, N., Olsen, A., Sabine, C. and Heimann, M.: Global](#)
1656 [surface-ocean pCO₂ and sea-Air CO₂ flux variability from an observation-driven ocean mixed-layer scheme,](#)
1657 [Ocean Sci., 9\(2\), 193–216, doi:10.5194/os-9-193-2013, 2013.](#)

1658

1659 [Rodgers, K. B., Aumont, O., Mikaloff Fletcher, S. E., Plancherel, Y., Bopp, L., De Boyer Montégut, C.,](#)
1660 [Iudicone, D., Keeling, R. F., Madec, G. and Wanninkhof, R.: Strong sensitivity of Southern Ocean carbon](#)
1661 [uptake and nutrient cycling to wind stirring, Biogeosciences, 11\(15\), 4077–4098, doi:10.5194/bg-11-4077-](#)
1662 [2014, 2014.](#)

1663

1664 [Rosso, I., Mazloff, M. R., Verdy, A. and Talley, L. D.: Space and time variability of the Southern Ocean carbon](#)
1665 [budget, J. Geophys. Res. Ocean., 122\(9\), 7407–7432, doi:10.1002/2016JC012646, 2017.](#)

1666

1667 [Roy, T., Bopp, L., Gehlen, M., Schneider, B., Cadule, P., Frölicher, T. L., Segsneider, J., Tjiputra, J., Heinze,](#)
1668 [C. and Joos, F.: Regional impacts of climate change and atmospheric CO₂ on future ocean carbon uptake: A](#)
1669 [multimodel linear feedback analysis, J. Clim., 24\(9\), 2300–2318, doi:10.1175/2010JCLI3787.1, 2011.](#)

1670

1671 [Sabine, C. L., Feely, R. A., Gruber, N., Key, R. M., Lee, K., Bullister, J. L., Wanninkhof, R., Wong, C. S., Wallace,](#)
1672 [D. W. R., Tilbrook, B., Millero, F. J., Peng, T. H., Kozyr, A., Ono, T. and Rios, A. F.: The oceanic sink for](#)
1673 [anthropogenic CO₂, Science \(80-. \), 305\(5682\), 367–371, doi:10.1126/science.1097403, 2004.](#)

1674

1675 [Sallée, J. B., Wienders, N., Speer, K. and Morrow, R.: Formation of subantarctic mode water in the](#)
1676 [southeastern Indian Ocean, Ocean Dyn., 56\(5–6\), 525–542, doi:10.1007/s10236-005-0054-x, 2006.](#)

1677 [Sallée, J. B., Shuckburgh, E., Bruneau, N., Meijers, A. J. S., Bracegirdle, T. J., Wang, Z. and Roy, T.:](#)
1678 [Assessment of Southern Ocean water mass circulation and characteristics in CMIP5 models: Historical bias](#)
1679 [and forcing response, J. Geophys. Res. Ocean., 118\(4\), 1830–1844, doi:10.1002/jgrc.20135, 2013.](#)

1680

1681 [Sarmiento, J. L. and Gruber, N.: Ocean Biogeochemical Dynamics, Carbon N. Y., 67, doi:10.1063/1.2754608,](#)
1682 [2006.](#)

1683

1684 [Sarmiento, J. L., Hughes, T. M. C., Stouffer, R. J. and Manabe, S.: Simulated response of the ocean carbon](#)
1685 [cycle to anthropogenic climate warming, Nature, 393\(6682\), 245–249, doi:10.1038/30455, 1998.](#)

1686 [Séférian, R., Bopp, L., Gehlen, M., Orr, J. C., Ethé, C., Cadule, P., Aumont, O., Salas y Mélia, D., Voldoire, A.](#)
1687 [and Madec, G.: Skill assessment of three earth system models with common marine biogeochemistry, Clim.](#)
1688 [Dyn., 40\(9–10\), 2549–2573, doi:10.1007/s00382-012-1362-8, 2013.](#)

V2 Changes 2018/3/6 6:53 PM

Formatted: normal, Right, Tabs: 7,62 cm, Centered + 15,24 cm, Right, Position:Horizontal: Left, Relative to: Column, Vertical: In line, Relative to: Margin, Wrap Around

V2 Changes 2018/3/6 6:53 PM

Formatted: Default Paragraph Font

1689
1690 [Segschneider, J. and Bendtsen, J.: Temperature-dependent remineralization in a warming ocean increases](#)
1691 [surface pCO₂ through changes in marine ecosystem composition, *Global Biogeochem. Cycles*, 27\(4\), 1214–](#)
1692 [1225, doi:10.1002/2013GB004684, 2013.](#)

1693
1694 [Son, S. W., Gerber, E. P., Perlwitz, J., Polvani, L. M., Gillett, N. P., Seo, K. H., Eyring, V., Shepherd, T. G.,](#)
1695 [Waugh, D., Akiyoshi, H., Austin, J., Baumgaertner, A., Bekki, S., Braesicke, P., Brühl, C., Butchart, N.,](#)
1696 [Chipperfield, M. P., Cugnet, D., Dameris, M., Dhomse, S., Frith, S., Garny, H., Garcia, R., Hardiman, S. C.,](#)
1697 [Jöckel, P., Lamarque, J. F., Mancini, E., Marchand, M., Michou, M., Nakamura, T., Morgenstern, O., Pitari,](#)
1698 [G., Plummer, D. A., Pyle, J., Rozanov, E., Scinocca, J. F., Shibata, K., Smale, D., Teyssdre, H., Tian, W. and](#)
1699 [Yamashita, Y.: Impact of stratospheric ozone on Southern Hemisphere circulation change: A multimodel](#)
1700 [assessment, *J. Geophys. Res. Atmos.*, 115\(19\), 1–18, doi:10.1029/2010JD014271, 2010.](#)

1701
1702 [Swart, N. C., Fyfe, J. C., Saenko, O. A. and Eby, M.: Wind-driven changes in the ocean carbon sink,](#)
1703 [Biogeosciences, 11\(21\), 6107–6117, doi:10.5194/bg-11-6107-2014, 2014.](#)

1704
1705 [Tagliabue, A., Mtshali, T., Aumont, O., Bowie, A. R., Klunder, M. B., Roychoudhury, A. N. and Swart, S.: A](#)
1706 [global compilation of dissolved iron measurements: Focus on distributions and processes in the Southern](#)
1707 [Ocean, *Biogeosciences*, 9\(6\), 2333–2349, doi:10.5194/bg-9-2333-2012, 2012.](#)

1708
1709 [Tagliabue, A., Williams, R. G., Rogan, N., Achterberg, E. P. and Boyd, P. W.: A ventilation-based framework](#)
1710 [to explain the regeneration-scavenging balance of iron in the ocean, *Geophys. Res. Lett.*, 41\(20\), 7227–](#)
1711 [7236, doi:10.1002/2014GL061066, 2014.](#)

1712
1713 [Takahashi, T., Olafsson, J., Goddard, J. G., Chipman, D. W. and Sutherland, S. C.: Seasonal variation of](#)
1714 [CO₂ and nutrients in the high-latitude surface oceans: A comparative study, *Global Biogeochem. Cycles*,](#)
1715 [7\(4\), 843–878, doi:10.1029/93GB02263, 1993.](#)

1716
1717 [Takahashi, T., Sutherland, S. C., Sweeney, C., Poisson, A., Metzl, N., Tilbrook, B., Bates, N., Wanninkhof, R.,](#)
1718 [Feely, R. A., Sabine, C., Olafsson, J. and Nojiri, Y.: Global sea-air CO₂ flux based on climatological surface](#)
1719 [ocean pCO₂, and seasonal biological and temperature effects, *Deep. Res. Part II Top. Stud. Oceanogr.*, 49,](#)
1720 [1601–1622, doi:10.1016/S0967-0645\(02\)00003-6, 2002.](#)

1721
1722 [Takahashi, T., Sutherland, S. C., Wanninkhof, R., Sweeney, C., Feely, R. A., Chipman, D. W., Hales, B.,](#)

V2 Changes 2018/3/6 6:53 PM

Formatted: normal, Right, Tabs: 7,62 cm, Centered + 15,24 cm, Right, Position: Horizontal: Left, Relative to: Column, Vertical: In line, Relative to: Margin, Wrap Around

V2 Changes 2018/3/6 6:53 PM

Formatted: Default Paragraph Font

1723 [Friederich, G., Chavez, F., Sabine, C., Watson, A., Bakker, D. C. E., Schuster, U., Metzl, N., Yoshikawa-Inoue,](#)
1724 [H., Ishii, M., Midorikawa, T., Nojiri, Y., Körtzinger, A., Steinhoff, T., Hoppema, M., Olafsson, J., Arnarson, T.](#)
1725 [S., Tilbrook, B., Johannessen, T., Olsen, A., Bellerby, R., Wong, C. S., Delille, B., Bates, N. R. and de Baar, H. J.](#)
1726 [W.: Climatological mean and decadal change in surface ocean pCO₂, and net sea-air CO₂ flux over the global](#)
1727 [oceans, Deep. Res. Part II Top. Stud. Oceanogr., 56\(8–10\), 554–577, doi:10.1016/j.dsr2.2008.12.009, 2009.](#)
1728
1729 [Takahashi, T., Sweeney, C., Hales, B., Chipman, D., Newberger, T., Goddard, J., Iannuzzi, R. and Sutherland,](#)
1730 [S.: The Changing Carbon Cycle in the Southern Ocean, Oceanography, 25\(3\), 26–37,](#)
1731 [doi:10.5670/oceanog.2012.71, 2012.](#)
1732
1733 [Taylor, K. E., Stouffer, R. J. and Meehl, G. A.: An overview of CMIP5 and the experiment design, Bull. Am.](#)
1734 [Meteorol. Soc., 93\(4\), 485–498, doi:10.1175/BAMS-D-11-00094.1, 2012.](#)
1735
1736 [Thomalla, S. J., Fauchereau, N., Swart, S. and Monteiro, P. M. S.: Regional scale characteristics of the](#)
1737 [seasonal cycle of chlorophyll in the Southern Ocean, Biogeosciences, 8\(10\), 2849–2866, doi:10.5194/bg-8-](#)
1738 [2849-2011, 2011.](#)
1739
1740 [Thompson, D. W. J., Solomon, S., Kushner, P. J., England, M. H., Grise, K. M. and Karoly, D. J.: Signatures of](#)
1741 [the Antarctic ozone hole in Southern Hemisphere surface climate change, Nat. Geosci., 4\(11\), 741–749,](#)
1742 [doi:10.1038/ngeo1296, 2011.](#)
1743
1744 [Visinelli, L., Masina, S., Vichi, M., Storto, A. and Lovato, T.: Impacts of data assimilation on the global ocean](#)
1745 [carbonate system, J. Mar. Syst., 158, 106–119, doi:10.1016/j.jmarsys.2016.02.011, 2016.](#)
1746
1747 [Wanninkhof, R., Asher, W. E., Ho, D. T., Sweeney, C. and McGillis, W. R.: Advances in Quantifying Air-Sea](#)
1748 [Gas Exchange and Environmental Forcing, Ann. Rev. Mar. Sci., 1\(1\), 213–244,](#)
1749 [doi:10.1146/annurev.marine.010908.163742, 2009.](#)
1750
1751 [Young, I. R.: Seasonal Variability of the Global Ocean Wind and Wave Climate, Int. J. Clim., 19\(July 2015\),](#)
1752 [931–950, doi:10.1002/\(SICI\)1097-0088\(199907\)19, 1999.](#)
1753
1754 [Zahariev, K., Christian, J. R. and Denman, K. L.: Preindustrial, historical, and fertilization simulations using a](#)
1755 [global ocean carbon model with new parameterizations of iron limitation, calcification, and N₂ fixation,](#)
1756 [Prog. Oceanogr., 77\(1\), 56–82, doi:10.1016/j.pocean.2008.01.007, 2008.](#)

V2 Changes 2018/3/6 6:53 PM

Formatted: normal, Right, Tabs: 7,62 cm, Centered + 15,24 cm, Right, Position: Horizontal: Left, Relative to: Column, Vertical: In line, Relative to: Margin, Wrap Around

V2 Changes 2018/3/6 6:53 PM

Formatted: Default Paragraph Font

1757
1758 [Zickfeld, K., Fyfe, J. C., Eby, M. and Weaver, A. J.: Comment on "Saturation of the southern ocean CO2](#)
1759 [sink due to recent climate change";, Science, 319\(5863\), 570; author reply 570,](#)
1760 [doi:10.1126/science.1146886, 2008.](#)

1761
1762
1763
1764
1765
1766
1767
1768
1769
1770
1771
1772
1773
1774
1775
1776
1777
1778
1779
1780
1781
1782
1783
1784
1785

V2 Changes 2018/3/6 6:53 PM
Formatted: Font:16 pt

V2 Changes 2018/3/6 6:53 PM
Formatted: normal, Widow/Orphan control, Adjust space between Latin and Asian text, Adjust space between Asian text and numbers

V2 Changes 2018/3/6 6:53 PM
Formatted: normal, Right, Tabs: 7,62 cm, Centered + 15,24 cm, Right, Position:Horizontal: Left, Relative to: Column, Vertical: In line, Relative to: Margin, Wrap Around

V2 Changes 2018/3/6 6:53 PM
Formatted: Default Paragraph Font

1786

1787

1788

Figures

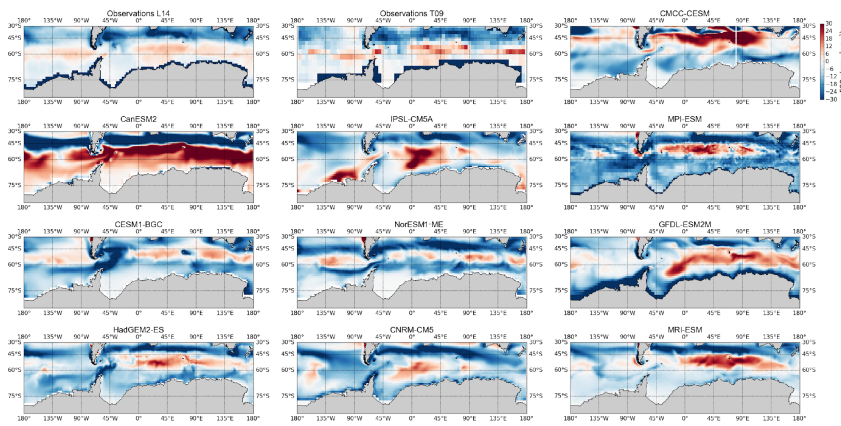


Fig. 1: Annual climatological Sea-Air CO₂ Flux (FCO₂, in gC m⁻² yr⁻¹) for observations (L14:Landschützer et al., 2014 and T09: Takahashi et al., 2009) and 10 CMIP5 models over 1995 – 2005.

1789

1790

1791

1792

1793

1794

1795

1796

1797

1798

1799

1800

1801

1802

V2 Changes 2018/3/6 6:53 PM
Formatted: Font:+Theme Headings, 16 pt

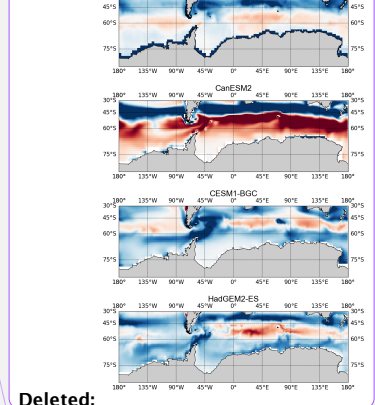
V2 Changes 2018/3/6 6:53 PM
Deleted:

V2 Changes 2018/3/6 6:53 PM
Formatted: normal

V2 Changes 2018/3/6 6:53 PM
Formatted: Font:+Theme Headings, 16 pt

V2 Changes 2018/3/6 6:53 PM
Formatted: Font:+Theme Headings

V2 Changes 2018/3/6 6:53 PM



Deleted:
V2 Changes 2018/3/6 6:53 PM
Formatted: Font:+Theme Headings

V2 Changes 2018/3/6 6:53 PM
Formatted: normal

V2 Changes 2018/3/6 6:53 PM
Deleted: ... [125]

V2 Changes 2018/3/6 6:53 PM
Formatted: ... [124]

V2 Changes 2018/3/6 6:53 PM
Formatted: Default Paragraph Font

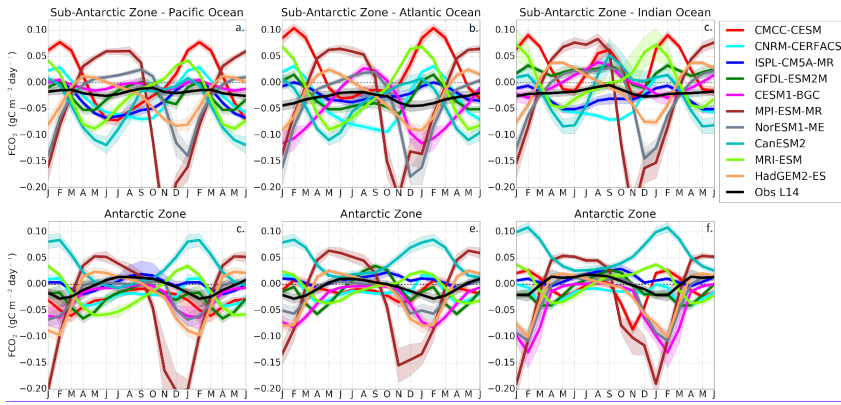


Fig. 2: Seasonal cycle of Sea-Air CO₂ Flux (FCO₂, in gC m⁻² yr⁻¹) in observations and 10 CMIP5 models in the Sub-Antarctic and Antarctic zones of the Pacific Ocean (first column), Atlantic Ocean (second column) and Indian Ocean (third column). The shaded area shows the temporal standard deviation over the considered period (1995 – 2005).

V2 Changes 2018/3/6 6:53 PM

Formatted: Font:+Theme Headings

V2 Changes 2018/3/6 6:53 PM

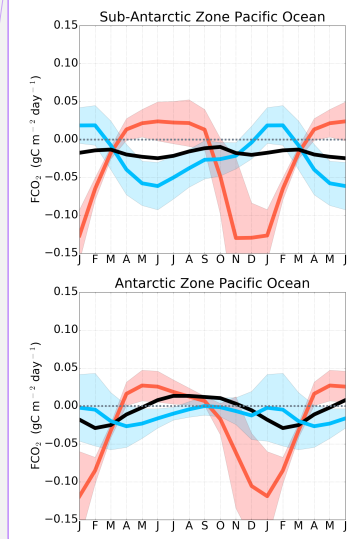
Formatted: normal

V2 Changes 2018/3/6 6:53 PM

Formatted: Font:+Theme Headings, 11 pt

V2 Changes 2018/3/6 6:53 PM

Deleted:



V2 Changes 2018/3/6 6:53 PM

Formatted: normal, Right, Tabs: 7,62 cm, Centered + 15,24 cm, Right, Position:Horizontal: Left, Relative to: Column, Vertical: In line, Relative to: Margin, Wrap Around

V2 Changes 2018/3/6 6:53 PM

Formatted: Default Paragraph Font

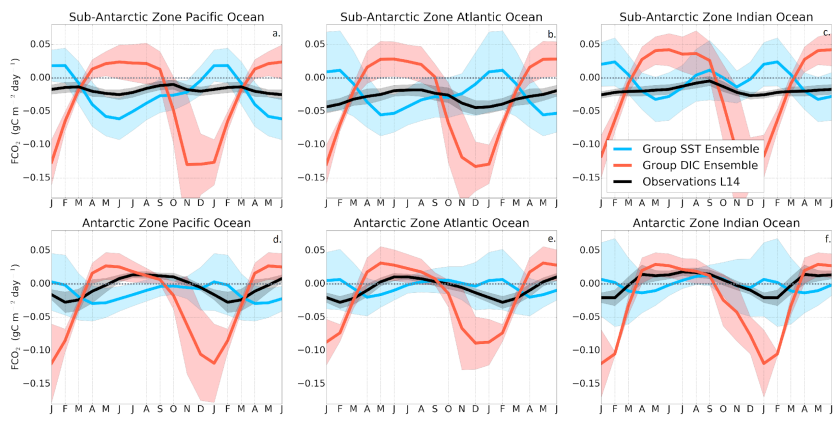


Fig. 3. Seasonal cycle of the equally weighted ensemble means of FCO_2 ($\text{gC m}^{-2} \text{yr}^{-1}$) from Fig. 2 for group DIC models (MPI-ESM, HadGEM-ES and NorESM), and group SST models (GFDL-ESM2M, CMCC-CESM, CNRM-CERFACS, IPSL-CM5A-MR, CESM1-BGC, NorESM2, MRI-ESM and CanESM2). The shaded areas show the ensemble standard deviation. The black line is the Landschützer et al., (2014) observations.

V2 Changes 2018/3/6 6:53 PM

Formatted: Font:+Theme Headings

V2 Changes 2018/3/6 6:53 PM

Deleted: -A

V2 Changes 2018/3/6 6:53 PM

Formatted: normal

V2 Changes 2018/3/6 6:53 PM

Formatted: Font:+Theme Headings

V2 Changes 2018/3/6 6:53 PM

Deleted: -B

V2 Changes 2018/3/6 6:53 PM

Formatted: Font:+Theme Headings

V2 Changes 2018/3/6 6:53 PM

Deleted: Landschützer et al., (2014)

V2 Changes 2018/3/6 6:53 PM

Formatted: Font:+Theme Headings

V2 Changes 2018/3/6 6:53 PM

Formatted: Font:+Theme Headings

V2 Changes 2018/3/6 6:53 PM

Formatted: normal, Right, Tabs: 7,62 cm, Centered + 15,24 cm, Right, Position:Horizontal: Left, Relative to: Column, Vertical: In line, Relative to: Margin, Wrap Around

V2 Changes 2018/3/6 6:53 PM

Formatted: Default Paragraph Font

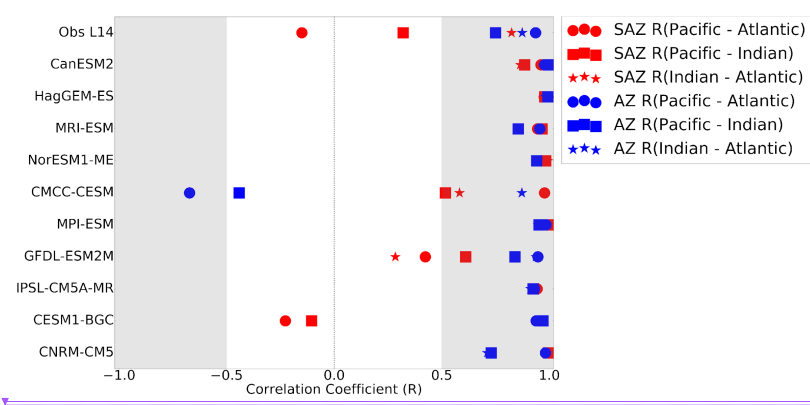
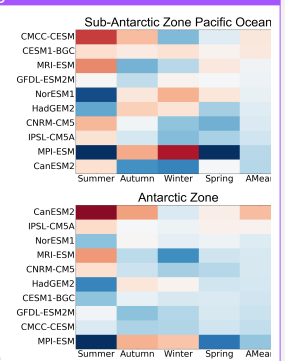


Fig. 4: The correlation coefficients (R) of basin – basin seasonal cycles of FCO₂ for observations (Landschützer et al., 2014) and 10 CMIP5 models in the three basins of the Southern Ocean i.e. Pacific, Atlantic and Indian basin.



Deleted:

V2 Changes 2018/3/6 6:53 PM
Formatted: Font:+Theme Headings

V2 Changes 2018/3/6 6:53 PM
Formatted: normal

V2 Changes 2018/3/6 6:53 PM
Deleted: Sea-Air CO₂ Flux mean

V2 Changes 2018/3/6 6:53 PM
Deleted: and annual biases with respect to

V2 Changes 2018/3/6 6:53 PM
Formatted: Font:+Theme Headings

V2 Changes 2018/3/6 6:53 PM
Formatted: Font:+Theme Headings

V2 Changes 2018/3/6 6:53 PM
Deleted: gC m⁻² yr⁻¹) for the Sub-/... [127]

V2 Changes 2018/3/6 6:53 PM
Formatted: Font:+Theme Headings

V2 Changes 2018/3/6 6:53 PM
Deleted: Pacific

V2 Changes 2018/3/6 6:53 PM
Formatted: Font:+Theme Headings

V2 Changes 2018/3/6 6:53 PM
Deleted: (first column, a and d),

V2 Changes 2018/3/6 6:53 PM
Formatted: Font:+Theme Headings

V2 Changes 2018/3/6 6:53 PM
Deleted: Ocean (second column, b and e)

V2 Changes 2018/3/6 6:53 PM
Formatted: Font:+Theme Headings

V2 Changes 2018/3/6 6:53 PM
Deleted: Ocean (third column, c a ... [128]

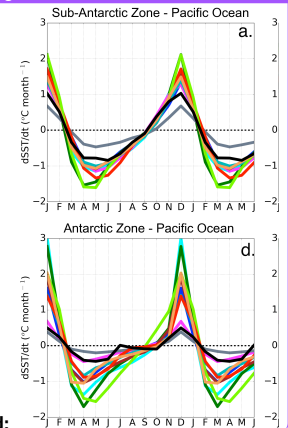
V2 Changes 2018/3/6 6:53 PM
Formatted: Font:+Theme Headings

V2 Changes 2018/3/6 6:53 PM
Deleted:

V2 Changes 2018/3/6 6:53 PM
Formatted: ... [126]

V2 Changes 2018/3/6 6:53 PM
Formatted: Default Paragraph Font

38



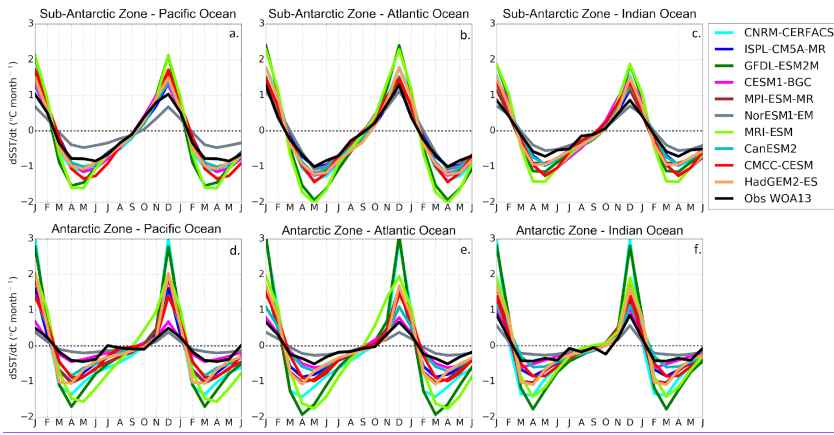


Fig. 5: Mean seasonal cycle of the estimated rate of change of sea surface temperature ($dSST/dt$, $^{\circ}C\ month^{-1}$) for the Sub-Antarctic and Antarctic zones of the Pacific Ocean (first column), Atlantic Ocean (second column) and Indian Ocean (third column).

V2 Changes 2018/3/6 6:53 PM

Formatted: Font:+Theme Headings, 11 pt

V2 Changes 2018/3/6 6:53 PM

Formatted: normal

V2 Changes 2018/3/6 6:53 PM

Formatted: Font:+Theme Headings

V2 Changes 2018/3/6 6:53 PM

Deleted: $\Delta SST/\Delta t$

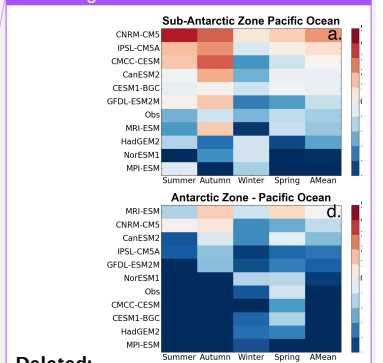
V2 Changes 2018/3/6 6:53 PM

Formatted: Font:+Theme Headings

V2 Changes 2018/3/6 6:53 PM

Formatted: Font:+Theme Headings, 11 pt

V2 Changes 2018/3/6 6:53 PM



Deleted:

V2 Changes 2018/3/6 6:53 PM

Formatted: normal, Right, Tabs: 7,62 cm, Centered + 15,24 cm, Right, Position:Horizontal: Left, Relative to: Column, Vertical: In line, Relative to: Margin, Wrap Around

V2 Changes 2018/3/6 6:53 PM

Formatted: Default Paragraph Font

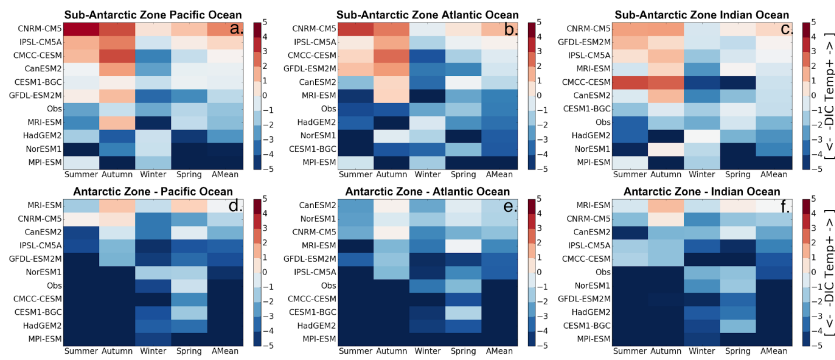
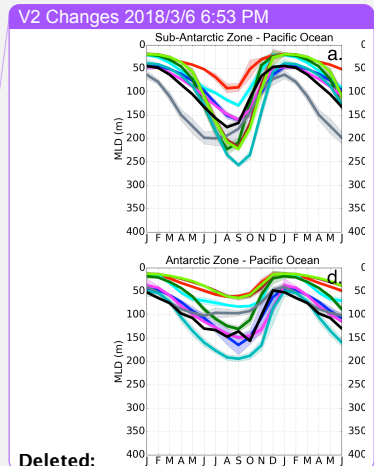
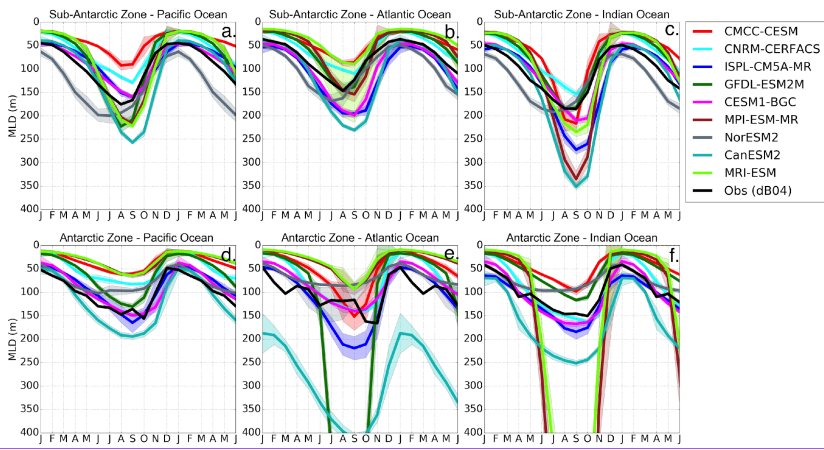


Fig. 6: Mean seasonal and annual values of the DIC-temperature control index (M_{T-DIC}). The increase in the red color intensity indicates increase in the strength of the temperature driver and the blue intensity shows the strength of the DIC driver. The models are sorted according to the annual mean value of the indicator presented in the last column (AMean)

- V2 Changes 2018/3/6 6:53 PM
Formatted: Font:+Theme Headings
- V2 Changes 2018/3/6 6:53 PM
Formatted: normal
- V2 Changes 2018/3/6 6:53 PM
Formatted: Font:+Theme Headings, Font color: Black
- V2 Changes 2018/3/6 6:53 PM
Formatted: Font:+Theme Headings, 11 pt, Font color: Black
- V2 Changes 2018/3/6 6:53 PM
Formatted: Font:+Theme Headings, Font color: Black

- V2 Changes 2018/3/6 6:53 PM
Formatted: normal, Right, Tabs: 7,62 cm, Centered + 15,24 cm, Right, Position:Horizontal: Left, Relative to: Column, Vertical: In line, Relative to: Margin, Wrap Around
- V2 Changes 2018/3/6 6:53 PM
Formatted: Default Paragraph Font



Deleted:

V2 Changes 2018/3/6 6:53 PM
Formatted: Font:+Theme Headings, Font color: Black

V2 Changes 2018/3/6 6:53 PM
Formatted: normal

V2 Changes 2018/3/6 6:53 PM
Formatted: Font:+Theme Headings

V2 Changes 2018/3/6 6:53 PM
Formatted: normal, Right, Tabs: 7,62 cm, Centered + 15,24 cm, Right, Position:Horizontal: Left, Relative to: Column, Vertical: In line, Relative to: Margin, Wrap Around

V2 Changes 2018/3/6 6:53 PM
Formatted: Default Paragraph Font

1939
 1940
 1941
 1942
 1943
 1944
 1945
 1946
 1947
 1948
 1949
 1950
 1951
 1952
 1953
 1954

Fig. 7: Seasonal cycle of the Mixed Layer Depth (MLD) in the Sub-Antarctic and Antarctic zones of the Pacific Ocean (first column), Atlantic Ocean (second column) and Indian Ocean (third column).

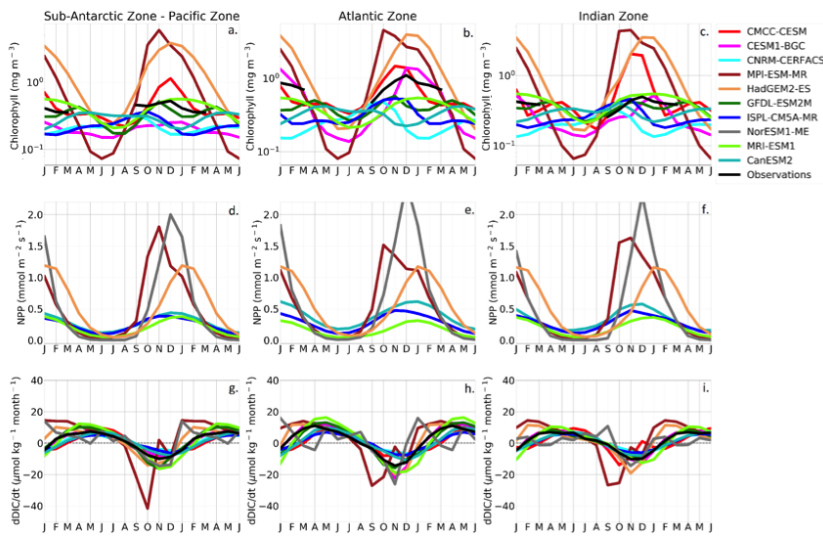


Fig. 8: The seasonal cycle of chlorophyll (mg m^{-3}), Net Primary Production ($\text{mmol m}^{-2} \text{s}^{-1}$) and the surface rate of change of DIC ($\mu\text{mol kg}^{-1} \text{month}^{-1}$) in the Sub-Antarctic zone of the Pacific Ocean (first column), Atlantic Ocean (second column) and Indian Ocean (third column).

V2 Changes 2018/3/6 6:53 PM

Deleted: - [129]

V2 Changes 2018/3/6 6:53 PM

Formatted: Font:+Theme Headings

V2 Changes 2018/3/6 6:53 PM

Formatted: normal

V2 Changes 2018/3/6 6:53 PM

Deleted: Estimated

V2 Changes 2018/3/6 6:53 PM

Deleted: entrainment fluxes (mol

V2 Changes 2018/3/6 6:53 PM

Formatted: Font:+Theme Headings

V2 Changes 2018/3/6 6:53 PM

Formatted: Font:+Theme Headings

V2 Changes 2018/3/6 6:53 PM

Formatted: Font:+Theme Headings

V2 Changes 2018/3/6 6:53 PM

Deleted: at the base of the mixed layer

V2 Changes 2018/3/6 6:53 PM

Formatted: Font:+Theme Headings

V2 Changes 2018/3/6 6:53 PM

Deleted: and Antarctic

V2 Changes 2018/3/6 6:53 PM

Formatted: Font:+Theme Headings

V2 Changes 2018/3/6 6:53 PM

Formatted: Font:+Theme Headings

V2 Changes 2018/3/6 6:53 PM

Formatted: normal, Right, Tabs: 7,62 cm,

Centered + 15,24 cm, Right,

Position:Horizontal: Left, Relative to:

Column, Vertical: In line, Relative to:

Margin, Wrap Around

V2 Changes 2018/3/6 6:53 PM

Formatted: Default Paragraph Font

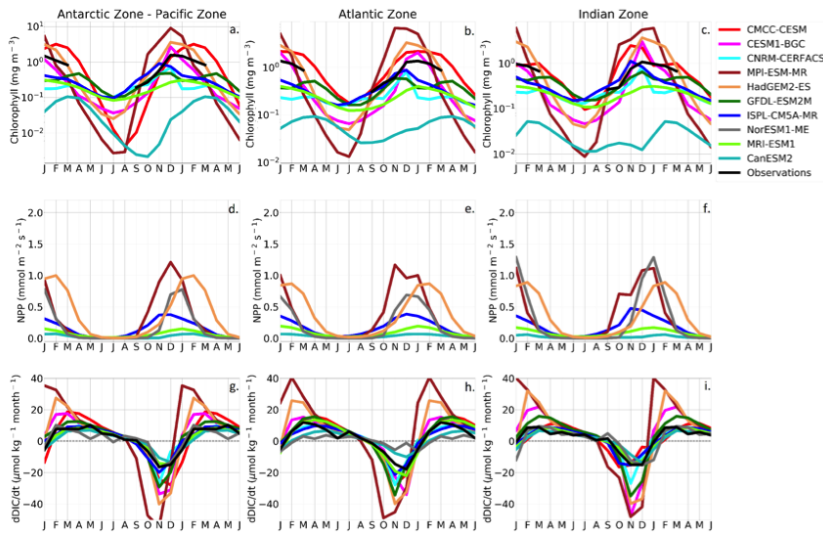


Fig. 9 Same as Fig. 8 for the Antarctic zone.

1972
1973
1974
1975

V2 Changes 2018/3/6 6:53 PM

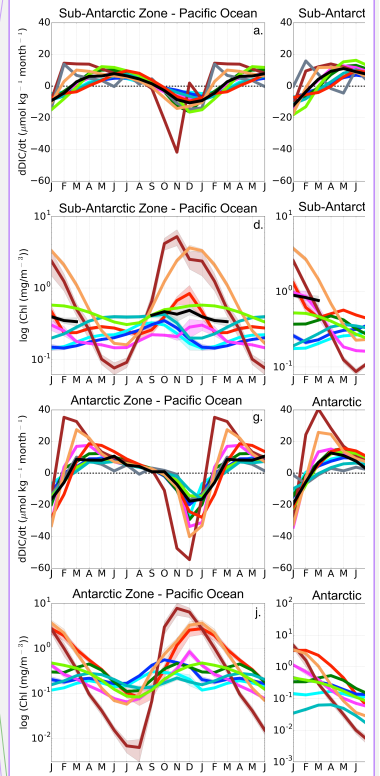
Moved (insertion) [5]

V2 Changes 2018/3/6 6:53 PM

Formatted: Font:+Theme Headings

V2 Changes 2018/3/6 6:53 PM

Deleted:



V2 Changes 2018/3/6 6:53 PM

Moved up [5]: Fig.

V2 Changes 2018/3/6 6:53 PM

Deleted: : Seasonal cycle of the rate of change of

V2 Changes 2018/3/6 6:53 PM

Formatted: Font:+Theme Headings

V2 Changes 2018/3/6 6:53 PM

Formatted: normal, Right, Tabs: 7,62 cm, Centered + 15,24 cm, Right, Position:Horizontal: Left, Relative to: Column, Vertical: In line, Relative to: Margin, Wrap Around

V2 Changes 2018/3/6 6:53 PM

Formatted: Default Paragraph Font

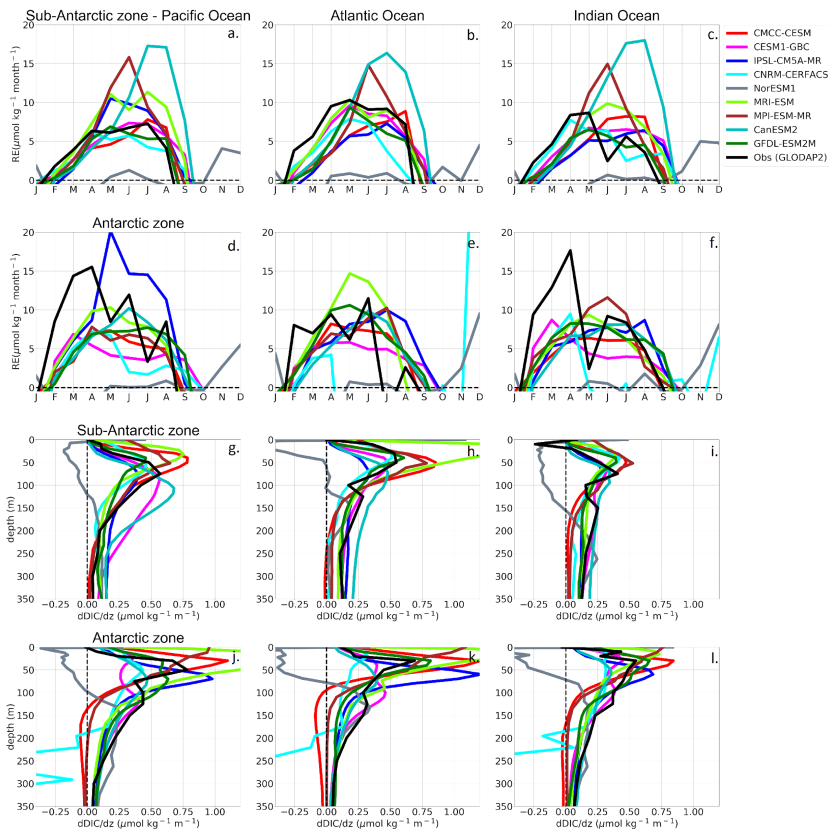


Fig. 10: (a-f) Estimated DIC entrainment fluxes ($\mu\text{mol kg}^{-1} \text{ month}^{-1}$) at the base of the mixed layer and (g-l) vertical DIC gradients ($\mu\text{mol kg}^{-1} \text{ m}^{-1}$) in the Sub-Antarctic and Antarctic zone of the Pacific Ocean (first column), Atlantic Ocean (second column) and Indian Ocean (third column).

- V2 Changes 2018/3/6 6:53 PM
Deleted: (μmol)
- V2 Changes 2018/3/6 6:53 PM
Deleted: and chlorophyll (mg m^{-3})
- V2 Changes 2018/3/6 6:53 PM
Formatted: Font:+Theme Headings
- V2 Changes 2018/3/6 6:53 PM
Deleted: surface ocean
- V2 Changes 2018/3/6 6:53 PM
Formatted: Font:+Theme Headings
- V2 Changes 2018/3/6 6:53 PM
Formatted: Font:+Theme Headings
- V2 Changes 2018/3/6 6:53 PM
Formatted: normal
- V2 Changes 2018/3/6 6:53 PM
Formatted: Font:+Theme Headings
- V2 Changes 2018/3/6 6:53 PM
Deleted: [130]
- V2 Changes 2018/3/6 6:53 PM
Formatted: Font:+Theme Headings, Not Bold
- V2 Changes 2018/3/6 6:53 PM
Formatted: Font:+Theme Headings, 14 pt
- V2 Changes 2018/3/6 6:53 PM
Formatted: Font:+Theme Headings, 12 pt, Not Bold
- V2 Changes 2018/3/6 6:53 PM
Formatted: Font:+Theme Headings, 16 pt
- V2 Changes 2018/3/6 6:53 PM
Formatted: normal, Right, Tabs: 7,62 cm, Centered + 15,24 cm, Right, Position:Horizontal: Left, Relative to: Column, Vertical: In line, Relative to: Margin, Wrap Around
- V2 Changes 2018/3/6 6:53 PM
Formatted: Default Paragraph Font

1998 | **Table 2:** Sea-Air CO₂ fluxes (Pg C yr⁻¹) annual mean uptake in the Southern Ocean (first column), here
1999 | defined as south of the Sub-tropical front, Sub-Antarctic zone (second column) and Antarctic zone (third
2000 | column). The third and forth column shows the Pattern Correlation Coefficient (PCC) and Root Mean
2001 | Square Error (RMSE) for the whole Southern Ocean for each model.

V2 Changes 2018/3/6 6:53 PM
Formatted: Font: +Theme Headings

V2 Changes 2018/3/6 6:53 PM
Formatted: normal, Right, Tabs: 7,62 cm, Centered + 15,24 cm, Right, Position: Horizontal: Left, Relative to: Column, Vertical: In line, Relative to: Margin, Wrap Around

V2 Changes 2018/3/6 6:53 PM
Formatted: Default Paragraph Font

Table 2: Sea-Air CO₂ Fluxes Mean Annual Uptake, PCC and RMSE

Model	Southern Ocean	Sub-Antarctic zone	Antarctic zone	PCC	RMSE
CNRM-CM5	-0.823 ± 0.003	-0.682 ± 0.002	-0.122 ± 0.001	0.44	17.9
GFDL-ESM2M	-0.161 ± 0.005	-0.074 ± 0.004	-0.077 ± 0.002	0.43	8.47
HadGEM2-ES	-0.489 ± 0.005	-0.284 ± 0.003	-0.197 ± 0.001	0.55	10.9
IPSL-CM5A-MR	-0.496 ± 0.003	-0.582 ± 0.006	0.101 ± 0.003	0.53	10.5
MPI-ESM-MR	-0.870 ± 0.006	-0.530 ± 0.002	-0.326 ± 0.002	0.37	9.87
MRI-ESM	-0.048 ± 0.002	0.022 ± 0.003	-0.070 ± 0.001	0.36	15.6
NorESM1	-0.699 ± 0.004	-0.412 ± 0.003	-0.270 ± 0.002	0.60	8.96
CESM1-BGC	-0.532 ± 0.006	-0.132 ± 0.003	-0.385 ± 0.004	0.47	9.15
CMCC-CESM	0.121 ± 0.006	0.367 ± 0.004	-0.225 ± 0.003	-0.09	17.9
CanESM2	-0.058 ± 0.008	-0.720 ± 0.006	0.661 ± 0.004	0.54	19.5
Observations	-0.253 ± 0.3	-0.296 ± 0.3	0.053 ± 0.3		

V2 Changes 2018/3/6 6:53 PM

Deleted: -

... [131]

V2 Changes 2018/3/6 6:53 PM

Formatted: normal, Right, Tabs: 7,62 cm, Centered + 15,24 cm, Right, Position:Horizontal: Left, Relative to: Column, Vertical: In line, Relative to: Margin, Wrap Around

V2 Changes 2018/3/6 6:53 PM

Formatted: Default Paragraph Font